



*Supplement of*

## **Significant influence of oxygenated volatile organic compounds on atmospheric chemistry: a case study in a typical industrial city in China**

**Jingwen Dai et al.**

*Correspondence to:* Kun Zhang (zk1231@shu.edu.cn) and Li Li (lily@shu.edu.cn)

The copyright of individual parts of the supplement might differ from the article licence.

## 7 Text S1 Adjustments of model parameter

8 The base parameter settings of the OBM were shown in Sec 2.2. As formal studies have  
9 reported, PKU-Mo as a catalytic converter for NO<sub>2</sub> measurement can cause interferences from other  
10 nitrogen–oxygen compounds (e.g., PAN, HNO<sub>3</sub>), which can lead to an overestimation NO<sub>2</sub> by  
11 30%~50% (Kim et al., 2015; Tan et al., 2017, 2019; Xu et al., 2013). In addition, strong  
12 anthropogenic emissions (such as vehicle emissions) around these sites, the model might not be able  
13 to reach the steady state resulting in positive deviation (Li et al., 2014). Therefore, the observed  
14 NO<sub>2</sub> concentrations among those 5 sites were reduced by 30%~40% (40% for ZL and CQ, 30% for  
15 CD, TZ and XD) to compensate for interferences from catalytic converter (Xu et al., 2013), and NO  
16 steady-state approximations (NO<sub>ss</sub>) was calculated (Equation (S1))(Del Negro et al., 1999; Jaeglé et  
17 al., 1994), which were then used for OBM inputs. Simulation constrained by all observed parameters  
18 including OVOCs and adjusted NO<sub>2</sub> and NO serves as the Base scenario. In order to investigate the  
19 impacts of model with OVOCs observationally constrained, scenario Free was conducted on top of  
20 the Base scenario by excluding observation constraints of OVOCs so that they were mainly  
21 generated by the oxidation of precursor VOCs in OBM. The time series plot of modeled and  
22 observed O<sub>3</sub> (Figure S6) and the model validation parameters were shown in Table S7. The modeled  
23 O<sub>3</sub> remain underestimate or overestimate at some times during the daytime, and significantly  
24 underestimate at night (Figure S6 (a)). This discrepancy may be due to the limitations of the 0-D  
25 model to express the transport processes in the atmosphere due to its simplification of atmospheric  
26 physical processes. The simplification of physical process is acceptable for modeling of in situ  
27 photochemistry.

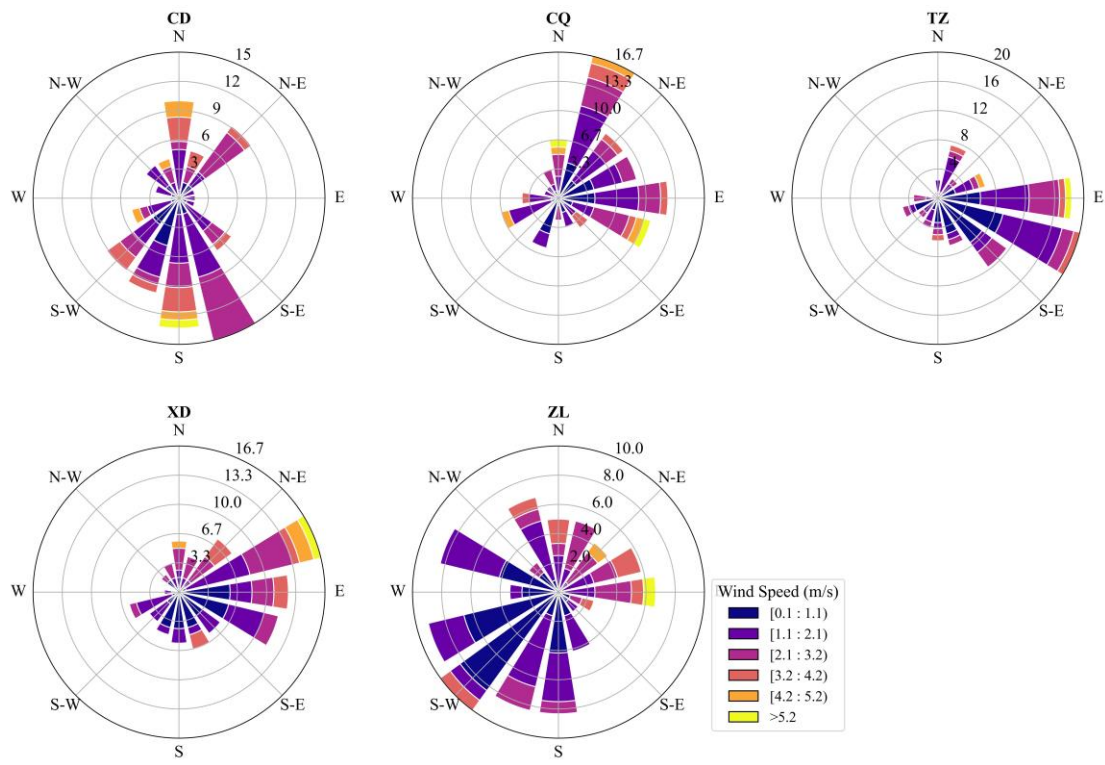


$$[NO_{ss}] = \frac{J_{NO_2} * [NO_2]}{k_{NO+O_3} * [O_3]} \quad (S1)$$

28 Where J<sub>NO<sub>2</sub></sub> represents the photolysis rate coefficient for reaction R1, k<sub>NO+O<sub>3</sub></sub> represents the reaction  
29 rate coefficient for the reaction R2, [NO<sub>ss</sub>], [NO<sub>2</sub>], and [O<sub>3</sub>] represents the mixing ratios of NO  
30 steady-state approximations, NO<sub>2</sub> and O<sub>3</sub>, respectively.

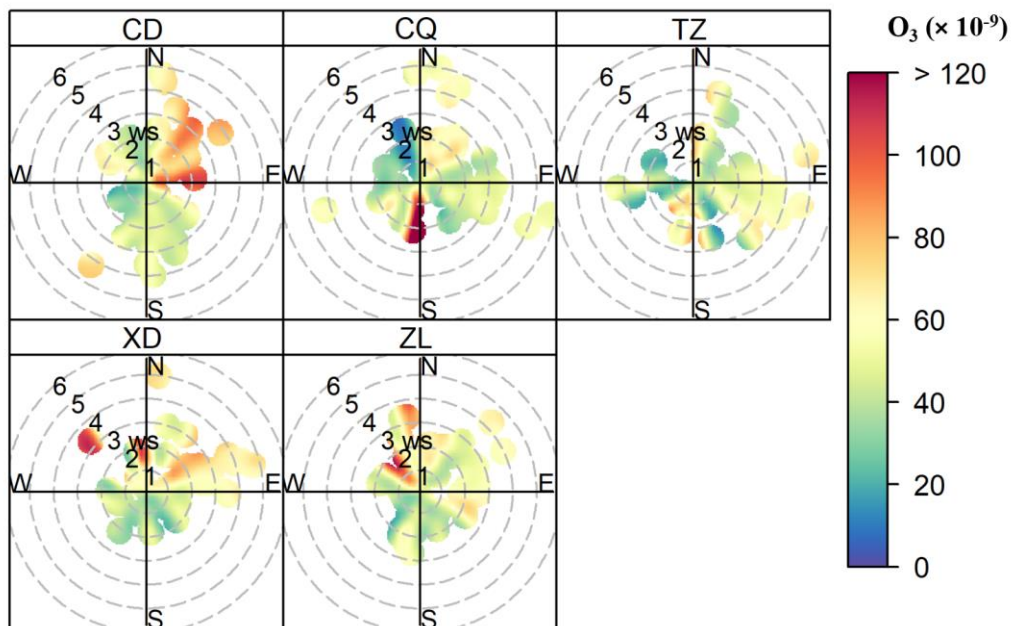
31 **Text S2 Simulations of OVOCs in the Free scenario**

32 Similar to Base scenario but without OVOCs observationally constraints in the Free scenario,  
33 the hourly average concentration of OVOCs at five sites was  $24.7 \pm 7.2 \times 10^{-9}$ , with a 59.1%  
34 overpredict of observations ( $15.5 \pm 11.3 \times 10^{-9}$ ). OVOCs at CD ( $18.7 \pm 4.1 \times 10^{-9}$ ), CQ ( $26.3 \pm 6.6 \times$   
35  $10^{-9}$ ), XD ( $24.7 \pm 7.0 \times 10^{-9}$ ), and ZL ( $32.1 \pm 6.2 \times 10^{-9}$ ) sites were overestimated in Free scenario by  
36 81.4%, 88.4%, 42.1%, and 126.5%, respectively. The OVOCs concentrations in the atmosphere are  
37 subject to a combination of emission/transport, chemical process, and deposition. Given that direct  
38 emissions of OVOCs are not considered in the Free scenario, the OVOCs concentrations in the  
39 model are determined by the chemical process and deposition. In terms of the chemical production  
40 process, it can be influenced by the emission of precursor VOCs indirectly. It has shown that in the  
41 presence of strong emission sources of VOCs, the model might not be able to reach an steady state,  
42 leading to a significant overestimation (Li et al., 2014). The observed OVOCs at TZ during August  
43 8 were unusually high due to transient emissions (Figure S6 (c)), pulling up the average levels.  
44 However, during the later days, the modeled OVOCs ( $15.5 \pm 10.7 \times 10^{-9}$ ) were also higher (15.3%)  
45 than the observed concentrations ( $13.4 \pm 11.5 \times 10^{-9}$ ) consisting with the other sites.



46

(b)

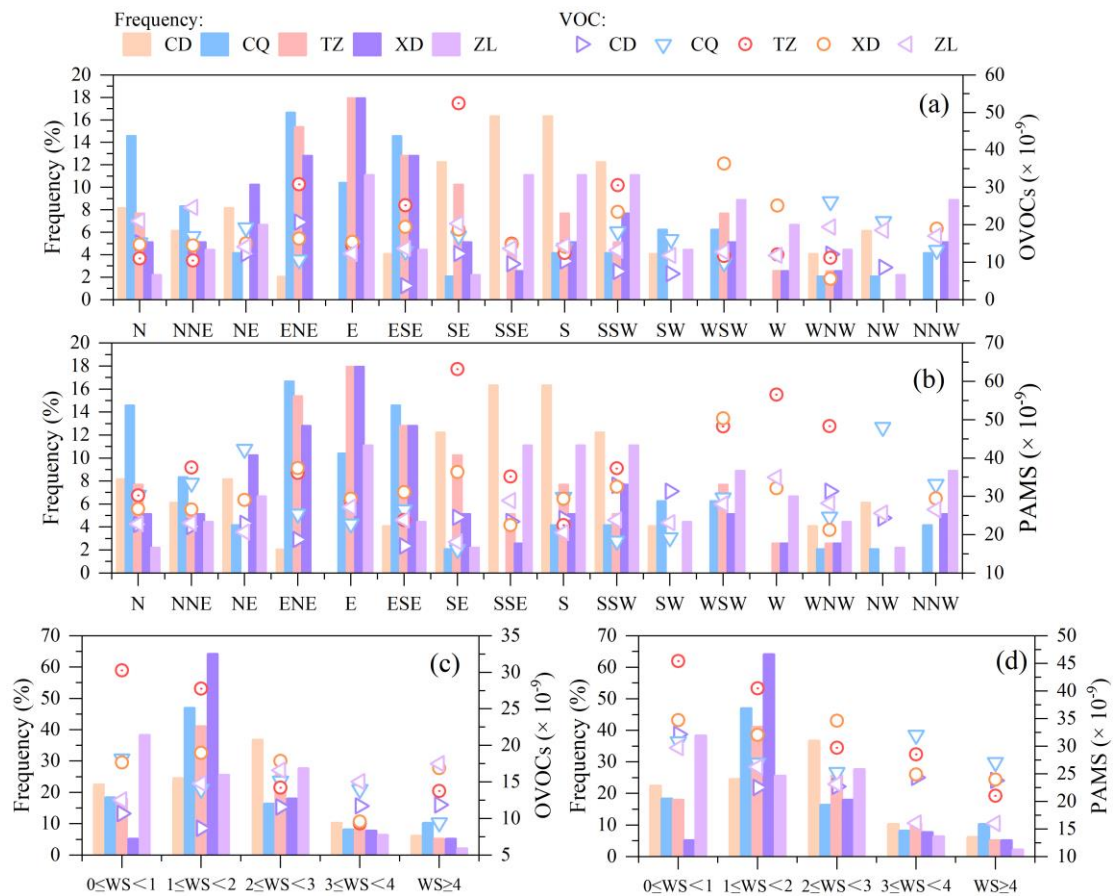


47

48

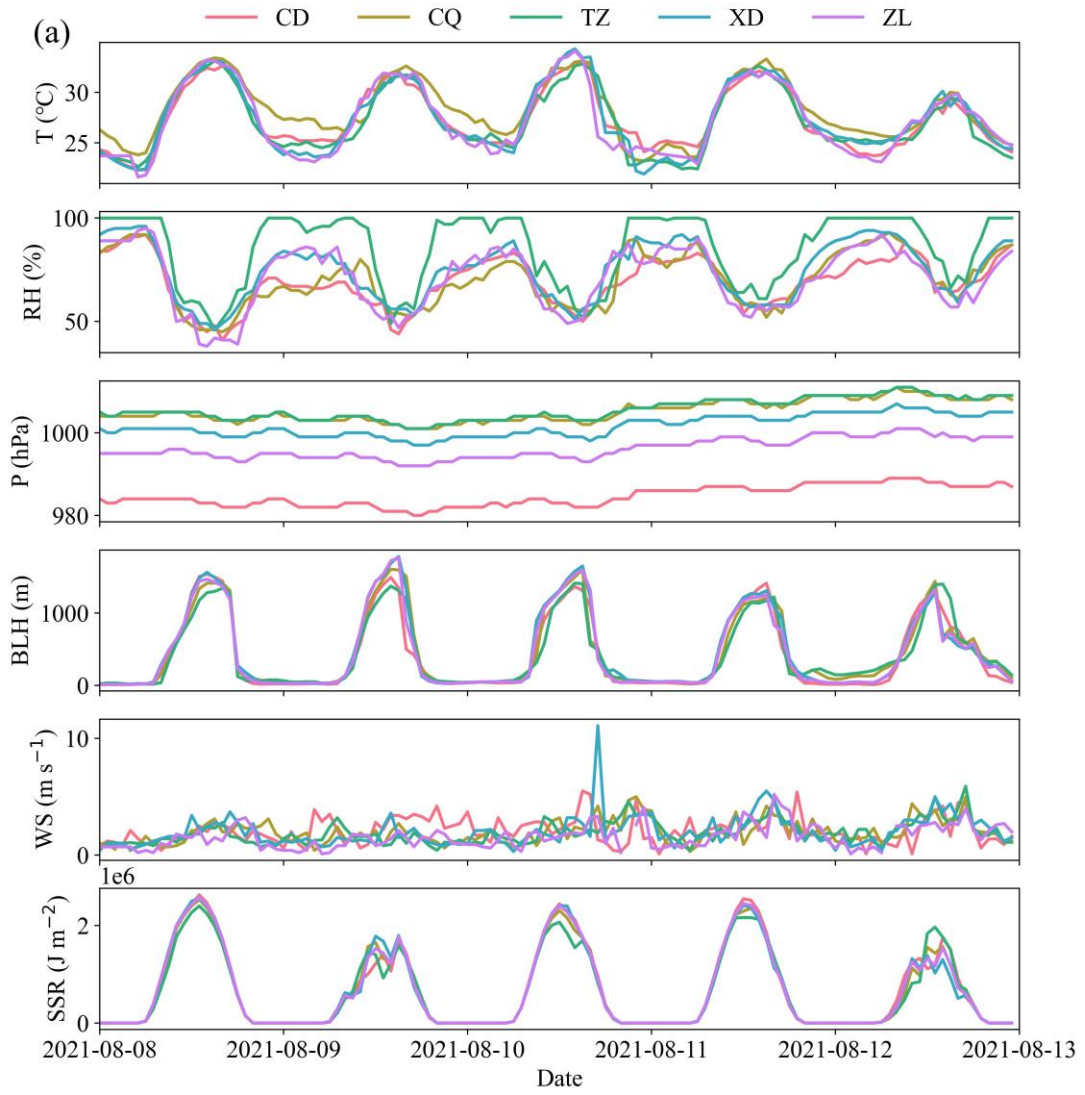
**Figure S1 (a) Wind rose and (b) O<sub>3</sub> pollution rose diagram of each site during the observation period.**

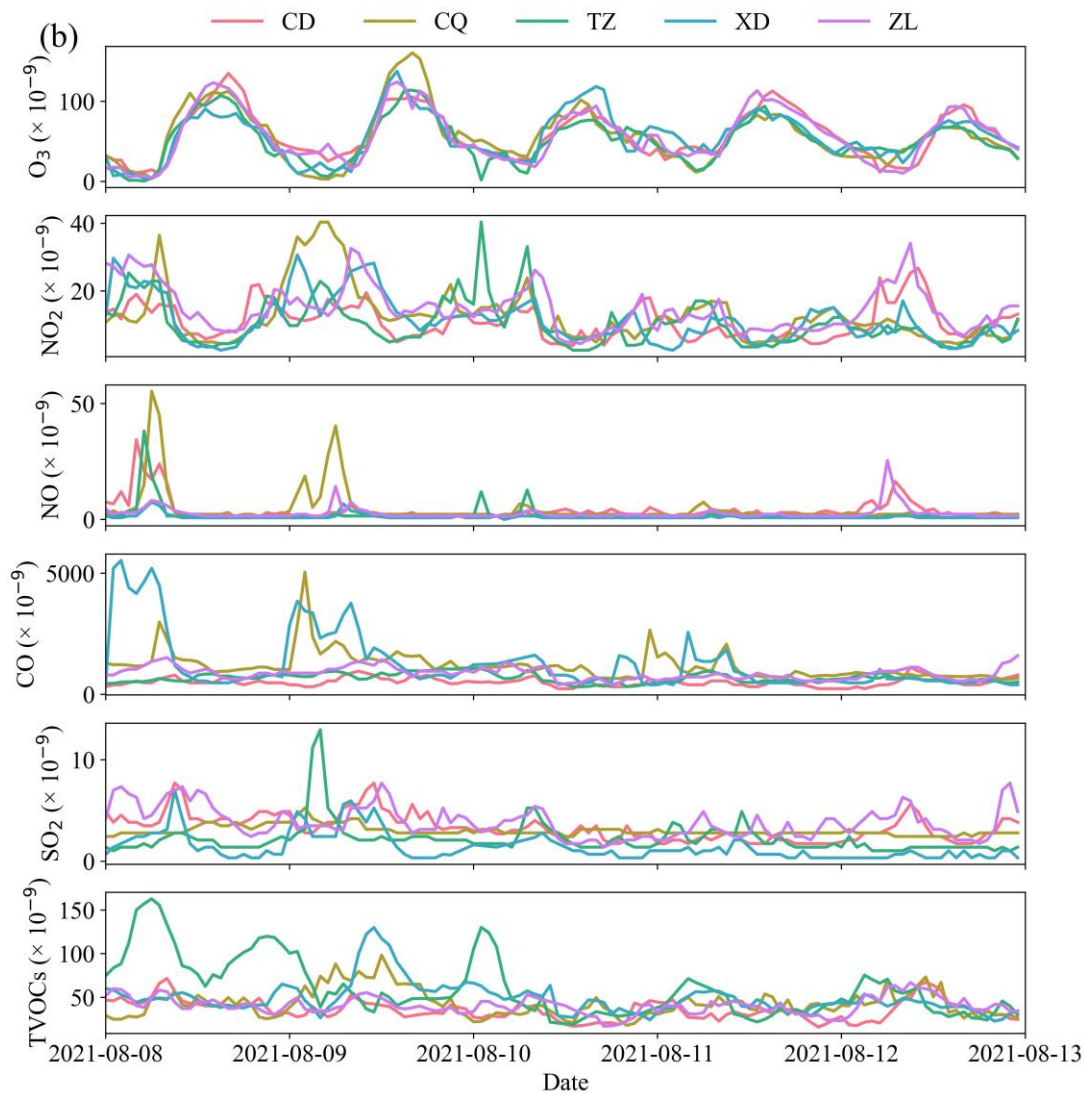
49



50

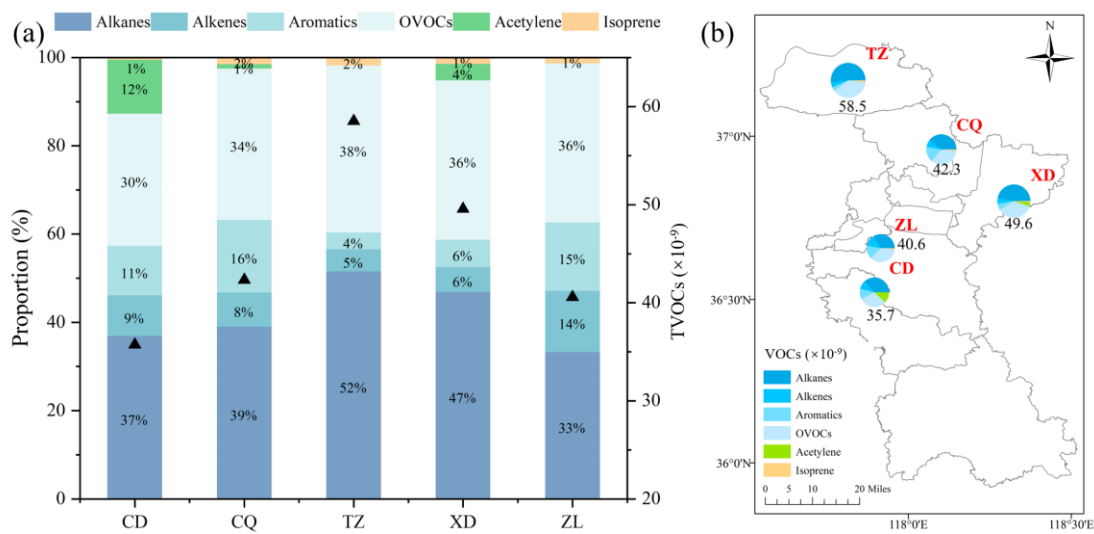
51 **Figure S2 Concentration statistics of OVOCs (a, c) and PAMS (b, d) at different wind speed**  
 52 **(WS) and wind direction (WD) intervals, respectively.**





54

55 **Figure S3 Time series of (a) meteorological parameters and (b) major pollutant mixing**  
 56 **ratios at five sites in Zibo.**

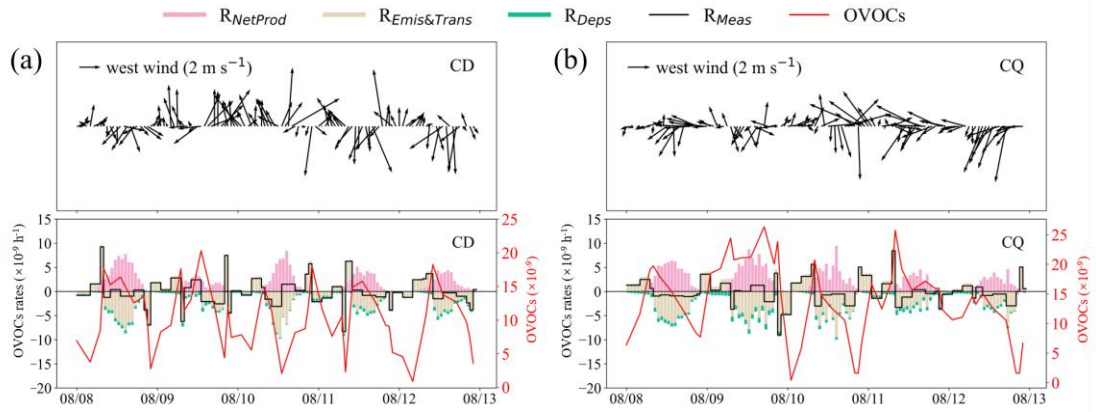


57

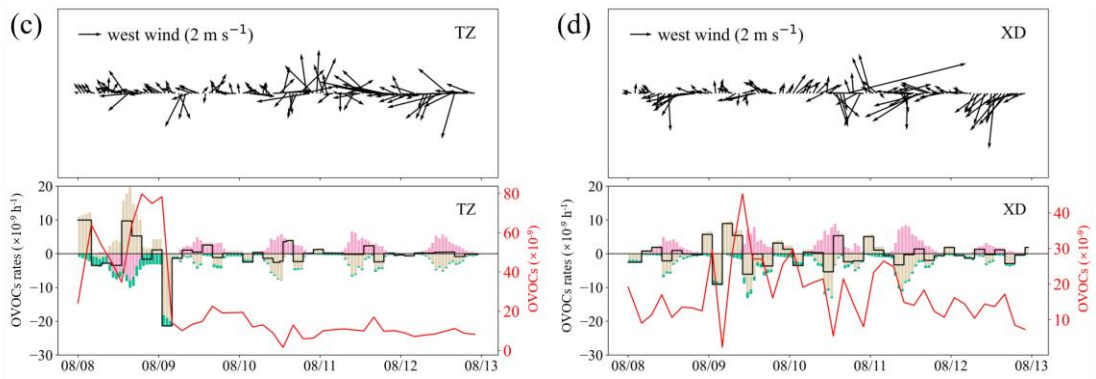
58 **Figure S4 (a) Comparison and (b) spatial distribution of VOCs components among five sites.**



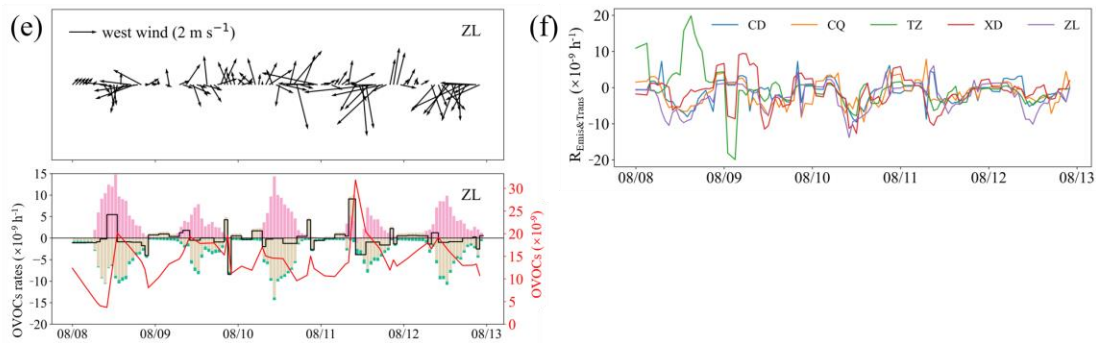
59



60

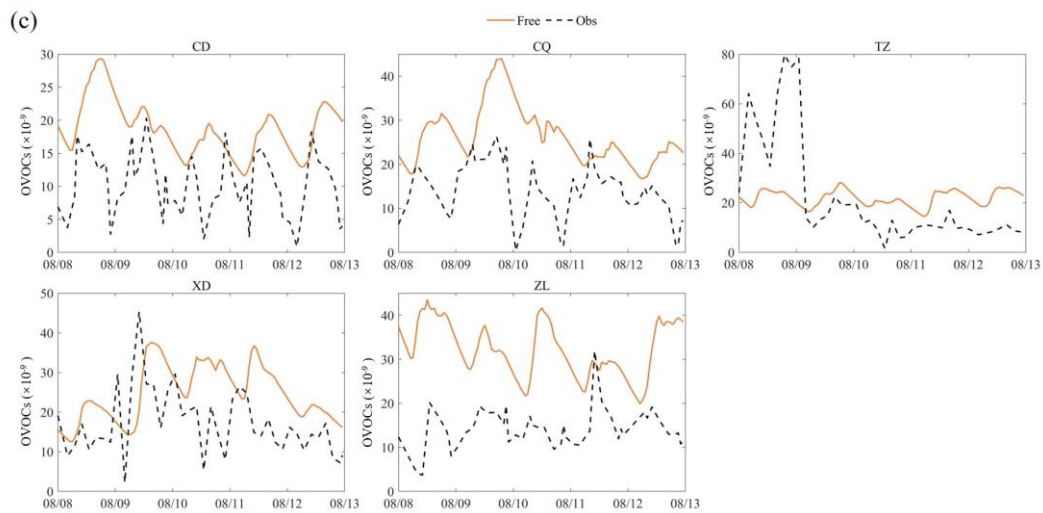
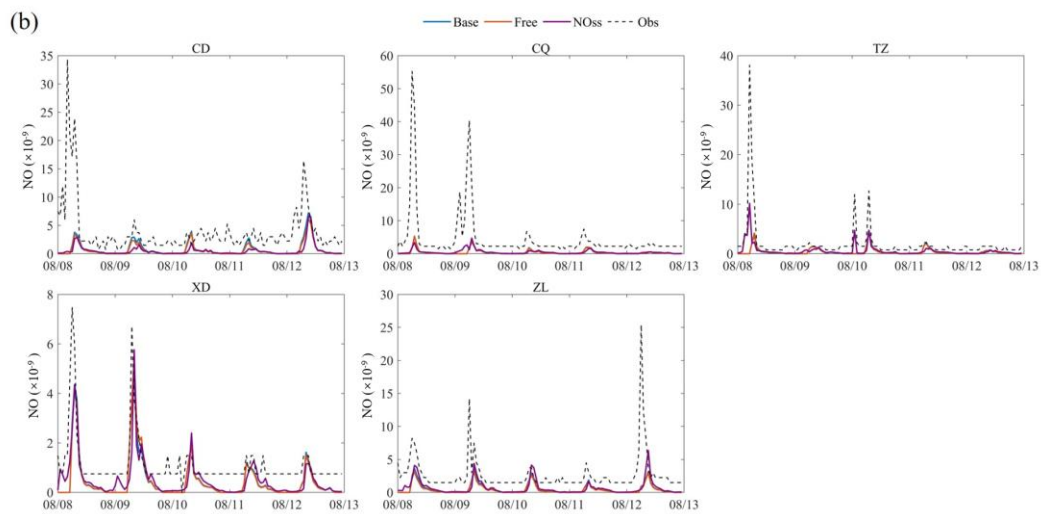
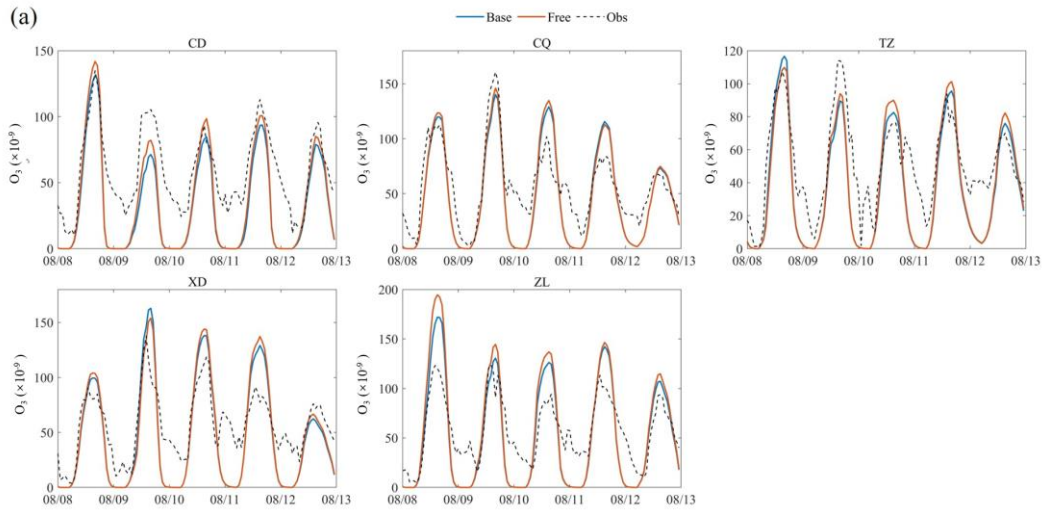


61

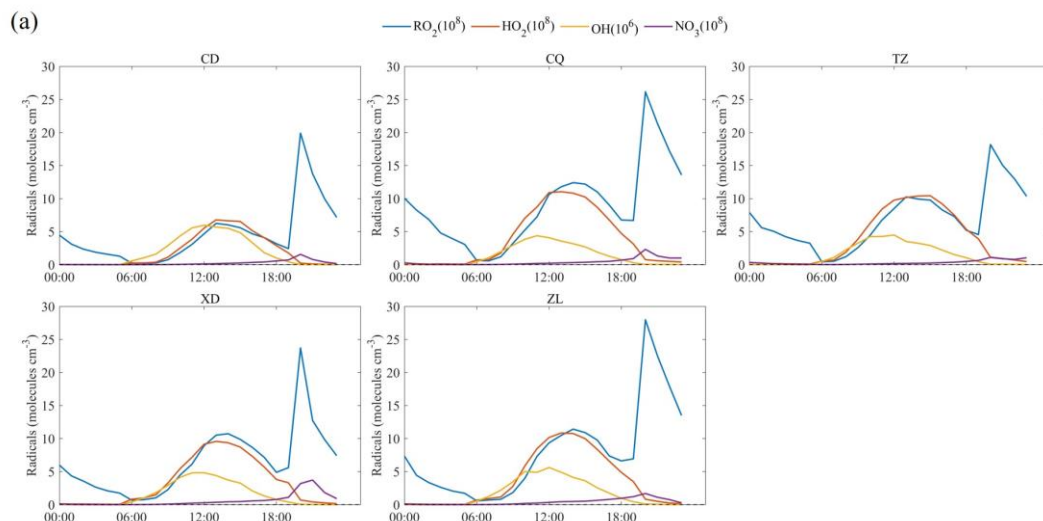


62 **Figure S5 OVOCs accumulation and contributions from local net photochemical production**  
 63 **and emissions/transport, and winds at (a) CD, (b) CQ, (c) TZ, (d) XD, and (e) ZL sites,**  
 64 **respectively, and (f) time variations of  $R_{\text{Emis\&Trans}}$  for all sites.  $R_{\text{NetProd}}$ ,  $R_{\text{Emis\&Trans}}$ ,  $R_{\text{Depos}}$  and**  
 65  **$R_{\text{Meas}}$  in the legend represent local net  $\text{O}_3$  photochemical production, emissions and regional**  
 66 **transport, deposition and observed OVOCs formation rates, respectively.**

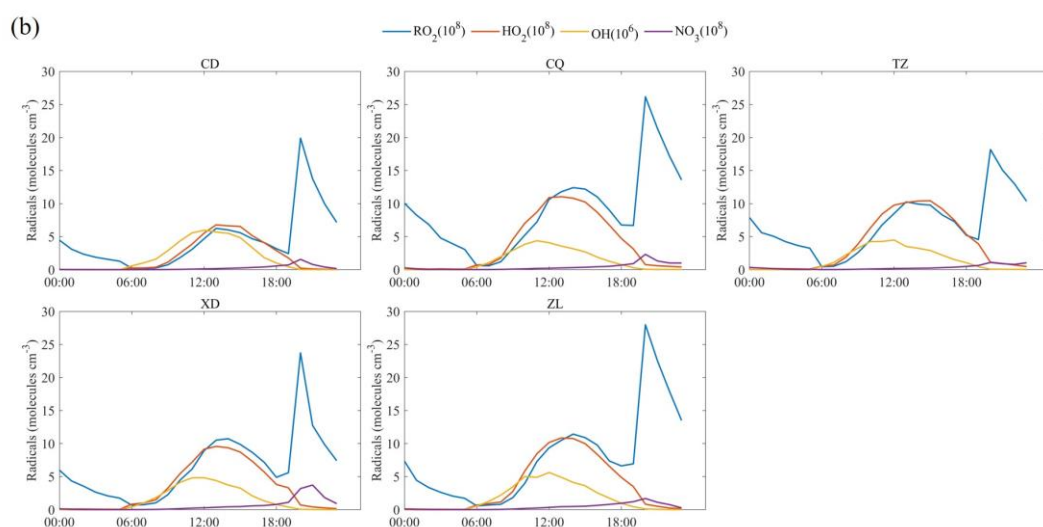




70 **Figure S6 Time series mixing ratios of  $O_3$ ,  $NO_x$  from observations (Obs), simulations (Base**  
 71 **and Free scenarios) and  $NO_{ss}$ , and that of OVOCs only including input**  
 72 **species from observation and Free scenario.**

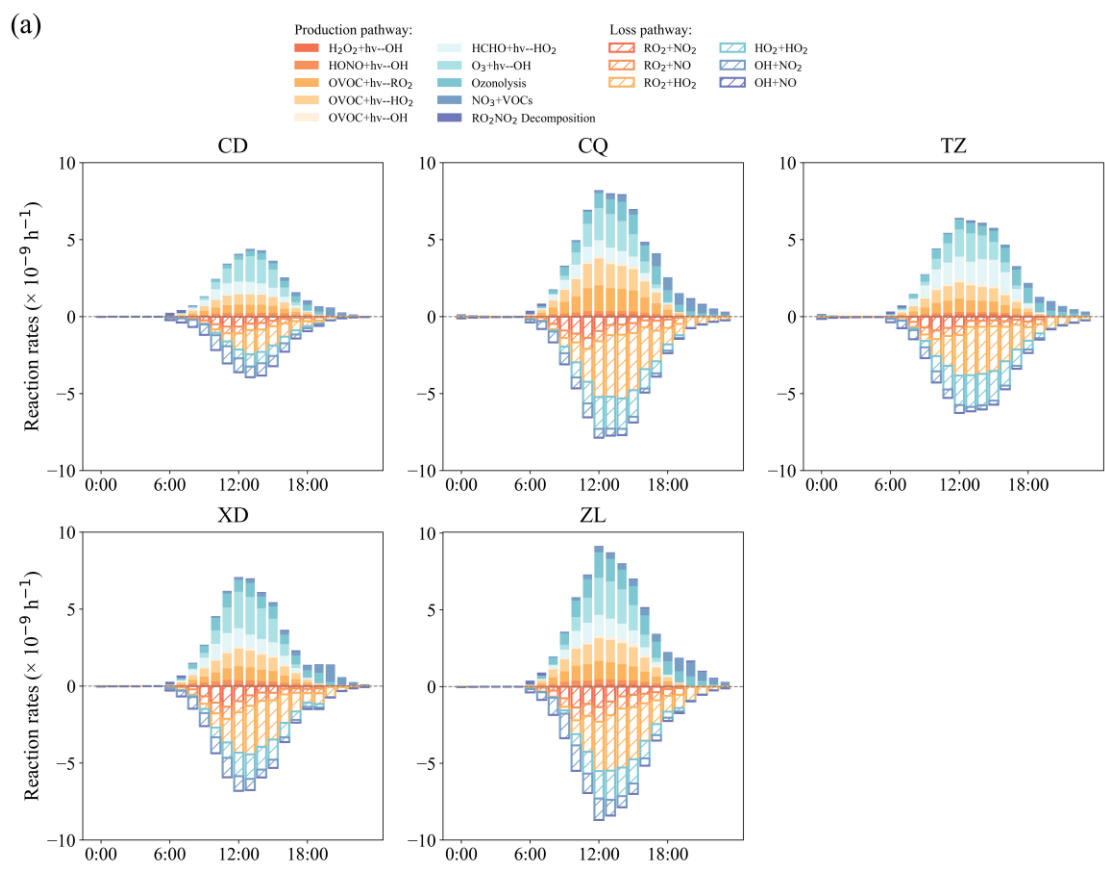


73

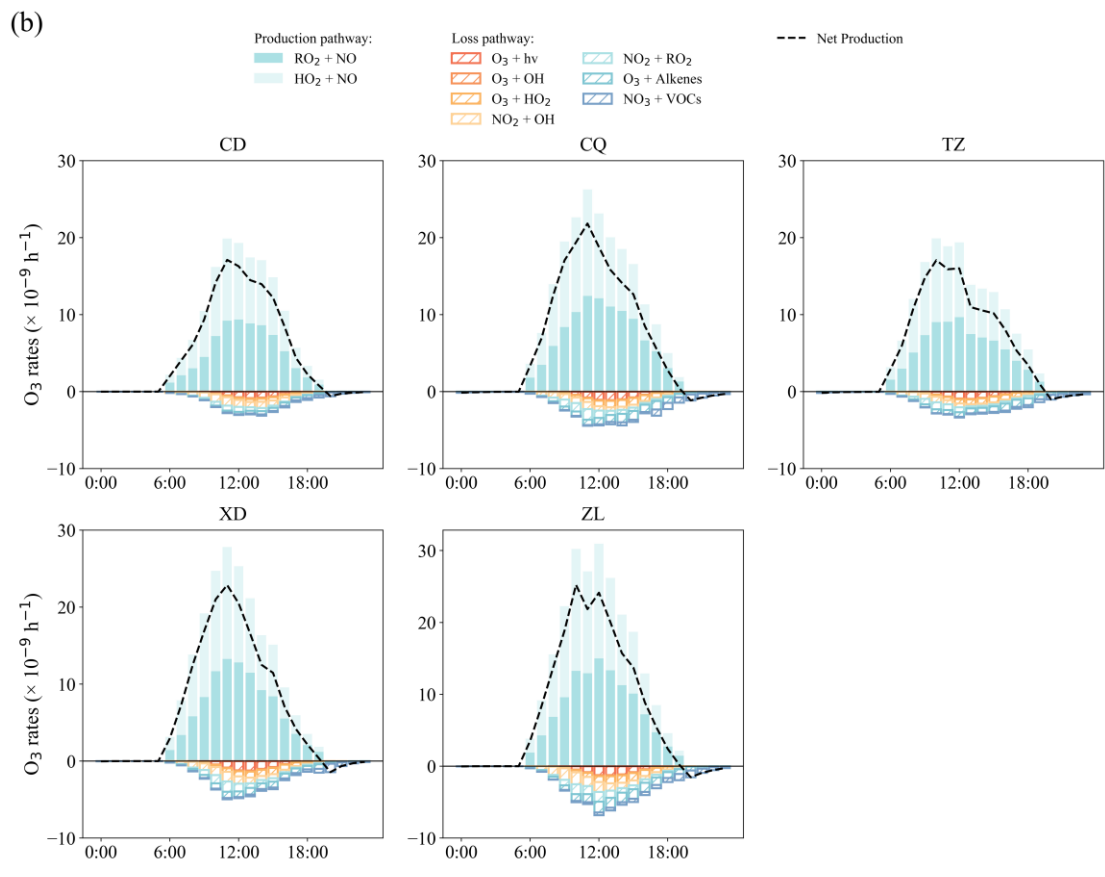


74

75 **Figure S7 (a) Simulated average daytime variation of ROx (RO<sub>2</sub>, HO<sub>2</sub>, and OH) and NO<sub>3</sub>**  
 76 **radicals at five sites, and (b) the effects of OVOCs observationally constrains on radical**  
 77 **concentrations, calculated by (Free – Base).**

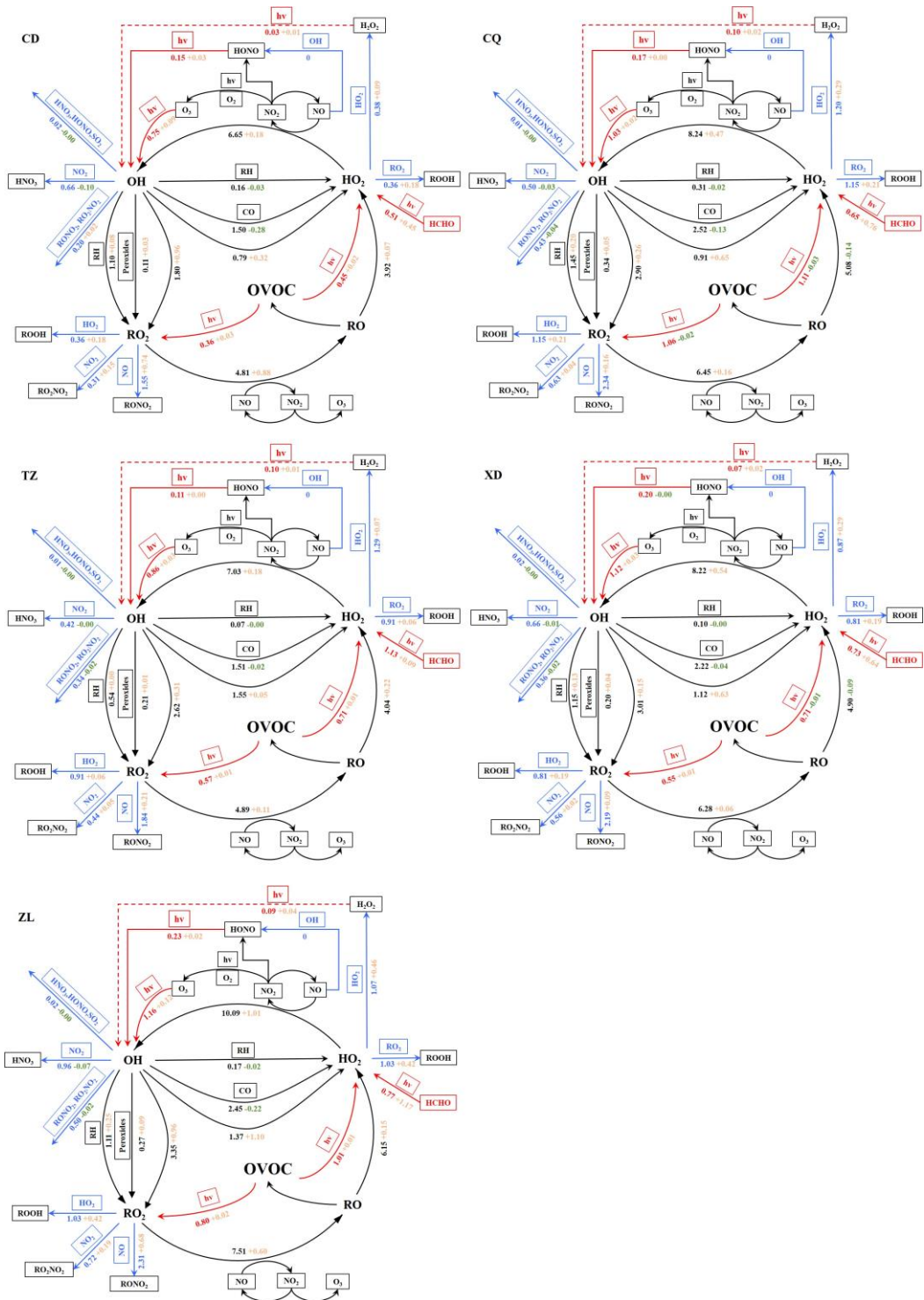


78



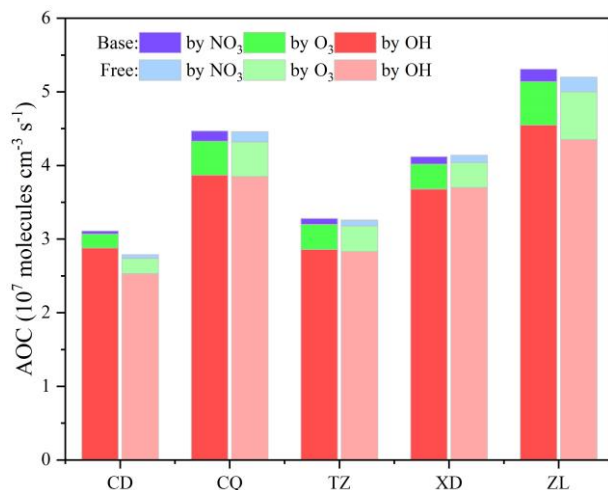
79

80 **Figure S8 Average diurnal profiles of sources and sinks of (a) RO<sub>x</sub> and (b) O<sub>3</sub> in the Base**  
 81 **scenario.**



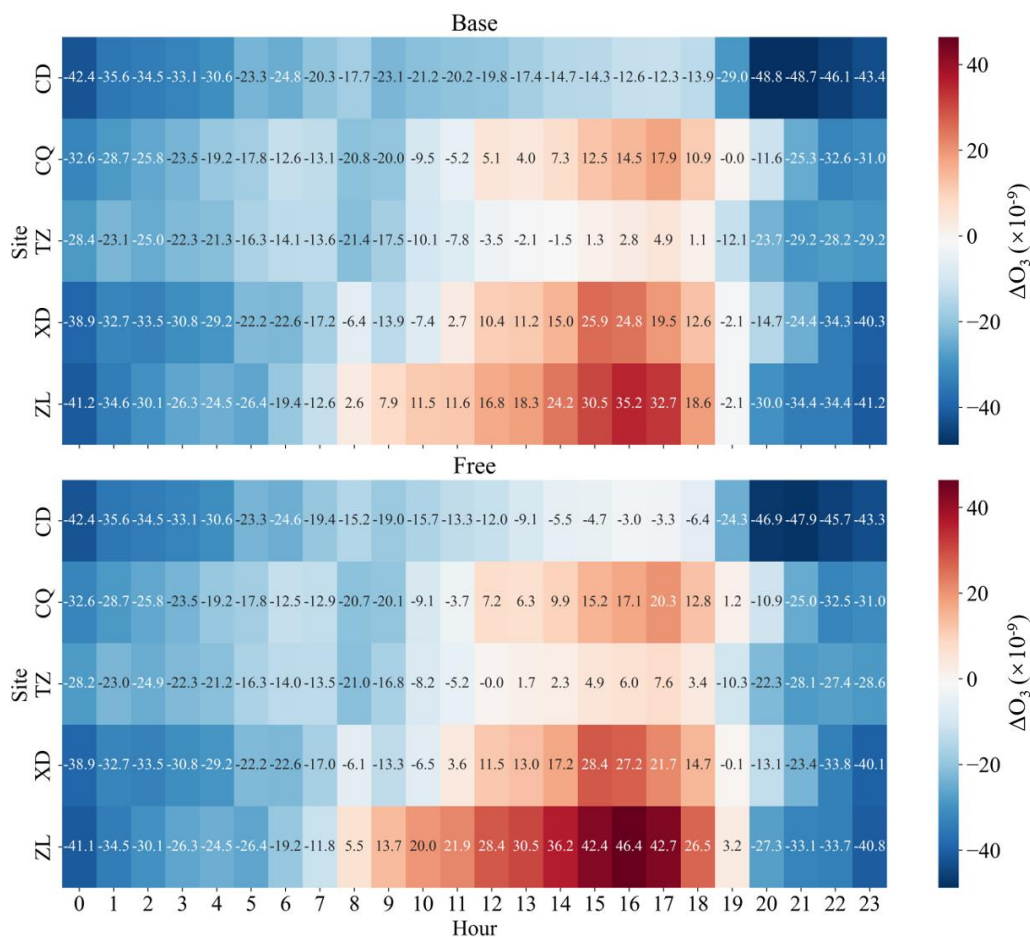
82

83 **Figure S9 Daytime (8:00-18:00 LT) average budgets of RO<sub>x</sub> radicals (in  $\times 10^{-9} \text{ h}^{-1}$ ) at each**  
 84 **site in Base scenario and the difference between Free and Base scenario. The first values**  
 85 **were the rates of Base, followed by the difference between Free and Base, where ‘-’ means**  
 86 **that the rate of Free scenario is lower than that of Base (in green), and conversely ‘+’ means**  
 87 **that the rate of Free is higher than that of Base (in orange). Primary RO<sub>x</sub> sources and sinks**  
 88 **are in red and blue, respectively, and the black lines represent the processes in RO<sub>x</sub> and NO<sub>x</sub>**  
 89 **recycling.**



90

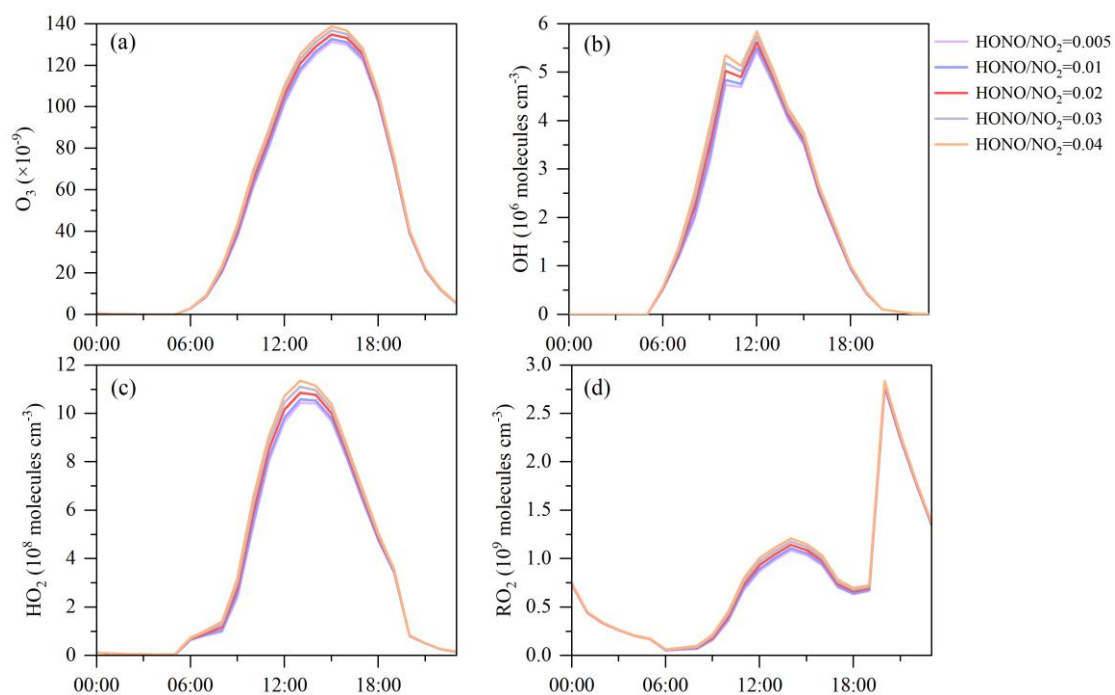
91 **Figure S10 Comparison of daytime (8:00-18:00 LT) atmospheric oxidation capacity (AOC)**  
 92 **between Base and Free scenario.**



93

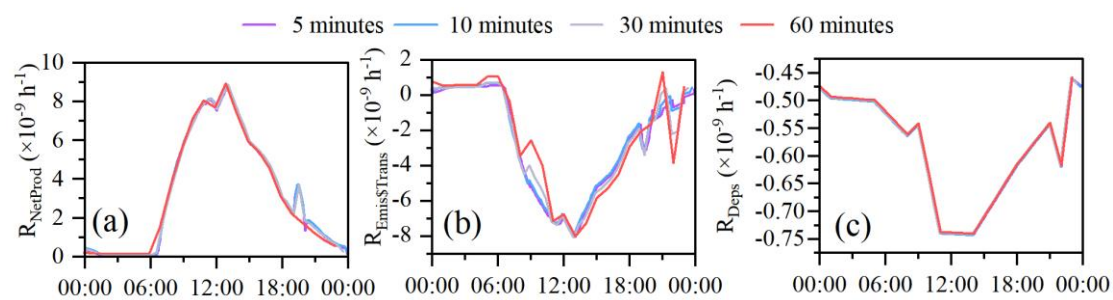
94 **Figure S11 Heat map of O<sub>3</sub> concentration difference ( $\Delta O_3 = \text{Sim} - \text{Obs}$ ) between simulated**  
 95 **and observed of Base and Free scenario**





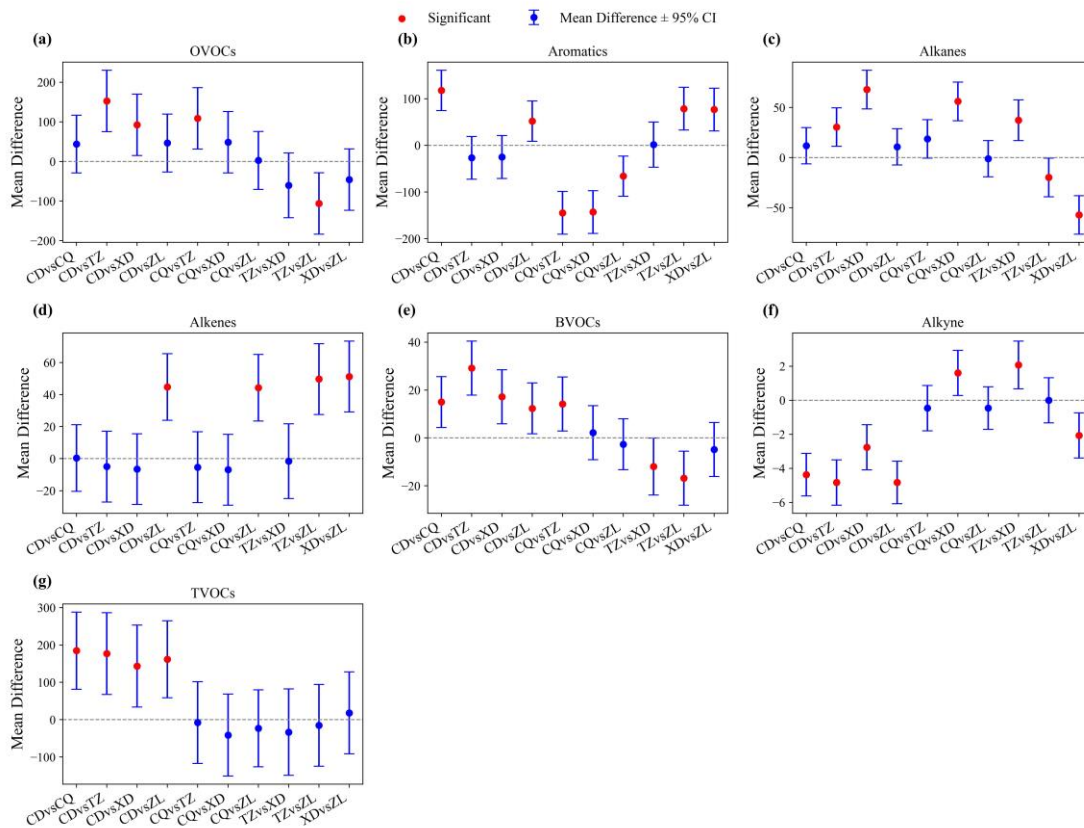
96

97 **Figure S12 Comparison of (a) O<sub>3</sub>, (b) HO<sub>2</sub>, (c) OH, (d) RO<sub>2</sub> concentrations under different**  
 98 **HONO/NO<sub>2</sub> ratios.**



99

100 **Figure S13 Comparison of R<sub>NetProd</sub>, R<sub>Emis&Trans</sub>, and R<sub>Dep</sub> contributed to OVOCs for different**  
 101 **time-step.**



102

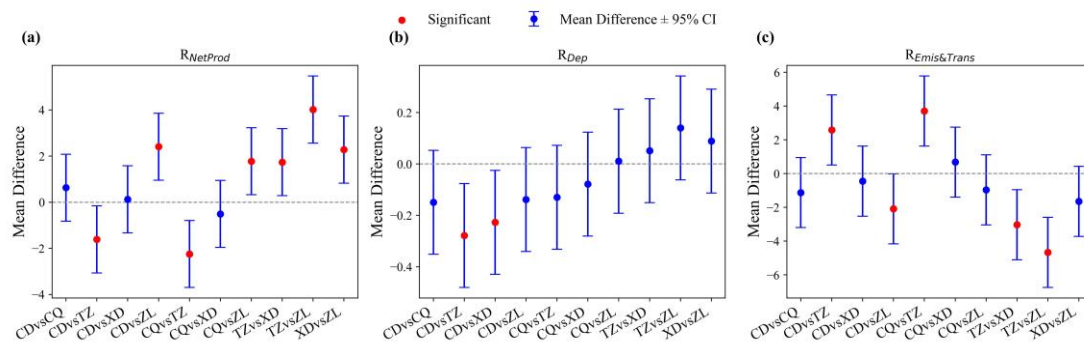
103

104

105

106

**Figure S14 Comparison of Tukey honestly significant difference (HSD) tests for OFP of VOC and its subclasses between different sites. Blue Dots represent the mean difference between the two sites, blue error bar represents the 95th percentile confidence interval (CI), red dots indicate significant difference between the two sites.**



107

108

109

**Figure S15 Tukey HSD tests for daytime (a)  $R_{NetProd}$ , (b)  $R_{Deps}$ , (c)  $R_{Emis&Trans}$  between sites.**



**Table S1 Location and site classification for the five different sites of Zibo**

Site name	Site	Longitude	Latitude	Style	Meteorological sites
Chengdong	CD	117°53'E	36°31'N	Downwind	Boshan
Chengqu	CQ	118°60'E	36°57'N	Upwind	Huantai
Tianzhen	TZ	117°48'E	37°10'N	Suburban	Gaoqing
Xindian	XD	118°19'E	36°48'N	Industrial	Linzi
Zhonglou	ZL	117°54'E	36°39'N	Urban	Zichuan

112

**Table S2 VOCs species and their names in Master Chemical Mechanism (MCMv3.3.1), minimum detection limits (MDL), and maximum incremental**

113

**reactivity coefficient (MIR). “—” means that the species is not listed in the mechanism.**

Species	MCM name	MDL ( $\times 10^{-9}$ )	MIR	Species	MCM name	MDL ( $\times 10^{-9}$ )	MIR
<b>Alkanes</b>				<b>BVOCs</b>			
Ethane	C2H6	0.079	0.28	Isoprene	C5H8	0.02	10.61
Propane	C3H8	0.046	0.49	<b>Alkynes</b>			
Isobutane	IC4H10	0.022	1.23	Acetylene	C2H2	0.032	0.95
n-Butane	NC4H10	0.027	1.15	<b>Aromatics</b>			
Cyclopentane	—	0.016	1.15	Benzene	BENZENE	0.012	0.72
Isopentane	IC5H12	0.087	2.39	Toluene	TOLUENE	0.013	4.00
n-Pentane	NC5H12	0.031	1.31	Ethylbenzene	EBENZ	0.014	3.04
2,2-Dimethylbutane	M22C4	0.014	1.17	m-Xylene	MXYL	0.027	9.75
2,3-Dimethylbutane	M23C4	0.019	0.97	Styrene	STYRENE	0.014	1.73
2-Methylpentane	M2PE	0.031	1.50	o-Xylene	OXYL	0.012	7.64
3-Methylpentane	M3PE	0.012	1.80	Isopropylbenzene	IPBENZ	0.014	2.52
n-Hexane	NC6H14	0.011	1.24	n-Propylbenzene	PBENZ	0.013	2.03
Methylcyclopentane	—	0.011	2.19	m-Ethyltoluene	METHTOL	0.032	7.39
2,4-Dimethylpentane	—	0.013	1.55	p-Ethyltoluene	PETHTOL	0.014	4.44
Cyclohexane	CHEX	0.016	1.25	1,3,5-Trimethylbenzene	TM135B	0.012	11.76
2-Methylhexane	M2HEX	0.012	1.19	1,2,4-Trimethylbenzene	TM124B	0.011	8.87
3-Methylhexane	M3HEX	0.013	1.61	1,2,3-Trimethylbenzene	TM123B	0.011	11.97
2,3-Dimethylpentane	—	0.013	1.34	o-Ethyltoluene	OETHTOL	0.013	5.59
2,2,4-Trimethylpentane	—	0.012	1.26	m-Diethylbenzene	—	0.011	7.10
n-Heptane	NC7H16	0.012	1.07	p-Diethylbenzene	—	0.011	4.43
Methylcyclohexane	—	0.011	1.70	<b>OVOCs</b>			

2,3,4-Trimethylpentane	—	0.013	1.03	Formaldehyde	HCHO	0.007	9.46
2-Methylheptane	—	0.013	1.07	Acetaldehyde	CH3CHO	0.016	6.54
3-Methylheptane	—	0.013	1.24	Acetone	CH3COCH3	0.009	0.36
n-Octane	NC8H18	0.012	0.90	Acrolein	ACR	0.008	7.45
n-Nonane	NC9H20	0.013	0.78	Propionaldehyde	C2H5CHO	0.026	7.08
n-Decane	NC10H22	0.011	0.68	Crotonaldehyde	C4ALDB	0.042	9.39
n-Undecane	NC11H24	0.018	0.61	Butanal	C3H7CHO	0.048	5.97
n-Dodecane	NC12H26	0.048	0.55	Benzaldehyde	BENZAL	0.055	-0.67
<b>Alkenes</b>				Cyclohexanone	CYHEXONE	0.058	1.35
Ethylene	C2H4	0.057	9.00	3-Methylbutyraldehyde	C3ME3CHO	0.058	4.97
Propylene	C3H6	0.022	11.66	Valeraldehyde	C4H9CHO	0.038	5.08
trans-2-Butene	TBUT2ENE	0.013	15.16	o-Tolualdehyde	OXYLAL	0.072	-0.59
1-Butene	BUT1ENE	0.023	9.73	m-Tolualdehyde	MXYLAL	0.089	-0.59
cis-2-Butene	CBUT2ENE	0.016	14.24	Hexaldehyde	C5H11CHO	0.060	4.35
trans-2-Pentene	TPENT2ENE	0.012	10.56	Heptaldehyde	C6H13CHO	0.034	3.69
1-Pentene	PENT1ENE	0.093	7.21	Octanal	—	0.029	3.16
cis-2-Pentene	CPENT2ENE	0.011	10.38	Nonanal	—	0.032	0.00
1-Hexene	HEX1ENE	0.014	5.49	Decanal	—	0.035	0.00

**Table S3 Uncertainty in sensitive model runs performed with different NO<sub>x</sub> settings**

Parameter	Site	Corrected [NO <sub>2</sub> ] <sup>a</sup> and [NO <sub>ss</sub> ] <sup>b</sup> (the Base scenario) (× 10 <sup>-9</sup> or × 10 <sup>-9</sup> h <sup>-1</sup> ) <sup>c</sup>	Changes based on the Base scenario				
			0.5*[NO <sub>2</sub> ]	0.6*[NO <sub>2</sub> ]	0.7*[NO <sub>2</sub> ]	[NO <sub>2</sub> ]	corrected [NO <sub>2</sub> ] and NO <sub>obs</sub> <sup>d</sup>
Daytime O <sub>3</sub>	CD	60.9	-6.9%	-2.8%	—	2.8%	5.3%
	CQ	82.4	-8.3%	—	7.4%	25.1%	19.2%
	TZ	66.2	-15.3%	-7.3%	—	18.2%	8.4%
	XD	85.2	-12.1%	-5.6%	—	12.0%	2.9%
	ZL	96.8	-5.9%	—	4.8%	13.9%	7.5%
Daytime R <sub>NetProd</sub>	CD	3.5	-10.2%	-4.4%	—	6.0%	8.7%
	CQ	4.1	-11.5%	—	10.3%	35.9%	27.1%
	TZ	1.9	-30.9%	-14.7%	—	36.7%	17.0%
	XD	3.6	-17.2%	-7.9%	—	17.4%	4.4%
	ZL	5.9	-7.2%	—	5.8%	17.1%	9.8%
R <sub>Emis&amp;Trans</sub>	CD	-1.3	-13.6%	-5.9%	—	8.2%	10.8%
	CQ	-1.5	-16.0%	—	14.5%	51.3%	37.6%
	TZ	-0.2	-122.4%	-58.1%	—	146.2%	67.2%
	XD	-1.2	-26.9%	-12.5%	—	28.1%	7.1%
	ZL	-2.5	-9.1%	—	7.5%	22.5%	12.2%

Note: <sup>a</sup> [NO<sub>2</sub>] represents the mixing ratios of NO<sub>2</sub>, the corrected [NO<sub>2</sub>] of CD, TZ and XD are 0.7\*[NO<sub>2</sub>], and those of CQ and ZL are 0.6\*[NO<sub>2</sub>] (Text S1). <sup>b</sup> NO<sub>ss</sub> and NO<sub>obs</sub><sup>d</sup> represent the mixing ratios of NO steady-state approximations and observed NO, respectively. <sup>c</sup> The × 10<sup>-9</sup> is for O<sub>3</sub>, and × 10<sup>-9</sup> h<sup>-1</sup> for R<sub>NetProd</sub> and R<sub>Emis&Trans</sub>.

**Table S4 Comparison of VOC mixing ratios and compositions in this study with former studies. Unit is 10<sup>-9</sup>.**

City	Site	Type	Period	Species	TVOCs	Alkanes	Alkenes	Aromatics	Acetylene	OVOCs	Halocarbons	References
Zibo	CD	Downwind	August 8-13, 2021	74	35.3	13.4	3.4	4.1	4.0	10.4		This study
	CQ	Upwind			42.6	16.9	3.9	7.5	0.5	13.9		
	TZ	Suburban			55.1	29.4	3.8	2.1	0.0	19.7		
	XD	Industrial			47.0	22.3	3.4	2.9	1.6	16.8		
	ZL	Urban			41.3	14.3	5.8	6.2	0.0	14.9		
	TZ	Suburban	High-O <sub>3</sub> episodes in July 2019	56	58.1	43.8	3.7	5.5	3.1		(Li et al., 2021)	
	BJ	Urban			23.8	13.8	3.2	3.7	2.4			
	XD	Suburban			38.1	22.5	7.8	3.4	3.2			
Qingdao		Rural	October 5 to November 10, 2018	106	7.6	4.7	1.6	0.6	0.2	0.4		(Liu et al., 2021a)
Rizhao		Urban	December 2021 to October 2022	111	19.7	8.6	2.1	1.4	0.7	4.0	3.6	(Zhang et al., 2023)
Jinan		Downtown	June 2010 to May 2012	55	25.3	14.3	7.0	4.0				(Wang et al., 2016)
Shanxi	LL	Urban	2019-2020	115	44.4	19.4	5.3	4.5	1.8	10.8	2.7	(Liu et al., 2023)
	LF				45.7	14.3	9.1	3.2	2.9	13.2	2.6	
	YC				37.5	13.9	5.9	2.4	3.1	9.6	2.7	
Beijing		Urban	2018	99	29.1	12.4	2.9	2.1	2.1	6.4	3.0	(Li et al., 2022)
Tianjing		Suburban	November 1, 2018 to March 15, 2019	54	30.6	17.3	6.5	3.9	2.9			(Gu et al., 2020)
Xianghe		Suburban	August 7-25, 2018	65	28.1	13.5	3.1	6.0		5.5		(Yang et al., 2021)
			December 1, 2018 to January 5, 2019		58.0	28.6	9.8	8.3		11.3		

City	Site	Type	Period	Species	TVOCs	Alkanes	Alkenes	Aromatics	Acetylene	OVOCs	Halocarbons	References
Wangdu	WD	Rural	2014 and 2016(June– July)	17	52.4					46.9		(Han et al., 2019)
Shenzhen	YMK	Rural			11.1						8.2	
Heshan		Suburban	October 20 to November 22, 2014	56	46.6	19.7	5.6	9.1		12.3		(Yang et al., 2017)
Beijing		Urban	August 10-27, 2013		50.4	23.8	5.6	9.1		11.9		
Zhengzhou		Urban	May 3-24, 2018	103	29.1	9.0	3.1	1.6		9.1	6.0	(Li et al., 2020)
Zhengzhou		Urban	July 2019	106	38.6	15.9	2.0	4.5	2.2	6.2	7.1	(Wang et al., 2022)
Xi'an		Whole city	June 20 to July 20, 2019	99	29.1	10.4	3.0	1.8	1.3	9.3	3.2	(Song et al., 2021)
Shanghai		Urban	2017.12.5-2018.1.15	113	63.6	26.2	6.8	7.3	3.2	14.9	5.1	(Liu et al., 2021b)
			March-May, 2019		25.0	15.0	3.0	1.6	2.0	1.7	1.7	
			June-August, 2019		20.0	9.5	2.6	1.5	1.4	3.0	1.9	
Ningde		Urban	September-November, 2019	94	22.4	12.2	2.3	1.9	1.4	2.1	2.5	(Chen et al., 2024)
			January-February, 2019		36.5	22.3	4.1	2.5	3.1	2.3	2.1	
	Mt. Wuyi	Background		70	6.1	1.9	1.1	1.3			1.8	
Fujian	XM	Urban	August-October 2016	70	17.9	9.1	2.1	4.1			2.6	(Hong et al., 2019)
	FZ	Urban		70	14.1	6.8	1.7	3.1			2.5	
	SZ-U	Urban	December 2017		35.7			8.6		26.2		
Shenzhen	NA-R	Regional	December 20, 2015 to January 15, 2016	18	13.5			4.1		8.7		(Huang et al., 2019)
	NL-B	Background	October 31, 2016 to November 14, 2016		8.2			0.9		6.5		

City	Site	Type	Period	Species	TVOCs	Alkanes	Alkenes	Aromatics	Acetylene	OVOCs	Halocarbons	References
Chongqing	JYS	Urban	August-September 2015	96	23.0	6.1	1.4	16.1	1.8	6.8	4.9	(Li et al., 2018)
	CJZ	Urban		96	49.9	17.7	7.1	5.8	5.2	7.6	4.8	
	NQ	Urban		96	34.1	12.9	4.1	4.6	3.8	5.1	3.1	
Chengdu		Urban	October 2016 to September 2017	55	41.8	23.6	8.2	7.2	2.7			(Song et al., 2018)
Chengdu		Whole city	May 2016 to January 2017	99	57.5	22.4	5.8	5.9	4.3	12.6	6.0	(Simayi et al., 2020)
Wuhan		Urban	January 2021	106	37.4	13.8	5.4	4.0	4.2	5.3	4.8	(Xu et al., 2023)
Wuhan		Urban	September 2016 to August 2017	102	34.7	15.9	4.2	3.2	2.4	4.9	3.7	(Hui et al., 2018)
Shenyang		Urban	August 20 to September 16, 2017	58	40.4	28.5	6.3	5.6		9.8		(Ma et al., 2019)



**Table S5 Measured mixing ratios, ozone formation potential from VOC species and groups.**

Species/Groups	VOC mixing ratios (mean±std) ( $\times 10^{-9}$ )					OFP (mean±std) ( $\mu\text{g m}^{-3}$ )				
	CD	CQ	TZ	XD	ZL	CD	CQ	TZ	XD	ZL
TVOCs	35.7±12.5	42.3±15.4	58.5±35.0	49.6±19.0	40.6±10.3	279.4±101.2	464.2±162.3	456.3±295.3	422.9±166.9	441.1±174.5
Alkanes	13.2±6.2	16.5±8.5	30.2±21.0	23.3±11.2	13.5±5.6	36.0±19.3	47.8±25.4	66.5±39.9	103.9±51.7	46.7±21.9
Alkenes	3.3±1.8	3.3±1.6	2.9±1.7	2.8±1.3	5.6±3.0	57.1±30.4	57.5±30.5	52.1±30.8	50.6±27.2	101.8±56.8
Aromatics	4.0±1.7	7.0±3.6	2.2±1.2	3.1±1.5	6.3±4.7	73.4±29.1	191.3±111.3	46.6±24.8	48.4±23.0	125.3±116.2
OVOCs	10.7±5.0	14.5±6.7	22.1±22.5	17.9±8.5	14.6±4.8	102.3±51.2	146.2±70.7	254.9±276.1	194.7±101.0	148.9±55.7
Acetylene	4.4±4.1	0.4±0.7	0.0±0.0	1.9±1.6	0.0±0.0	4.8±4.5	0.5±0.8	0.0±0.1	2.1±1.7	0.0±0.1
Isoprene	0.2±0.2	0.6±0.6	1.1±0.8	0.7±0.5	0.6±0.7	5.8±7.7	20.8±17.8	34.9±25.8	23.0±16.3	18.1±23.6
Benzene	1.0±0.5	0.3±0.2	0.2±0.3	1.1±0.6	1.2±0.5	2.4±1.3	0.6±0.4	0.4±0.7	2.7±1.5	3.0±1.3
Toluene	1.2±0.5	1.2±0.9	1.4±1.0	0.9±0.5	1.6±1.3	19.3±7.5	20.0±15.2	23.6±15.9	14.5±8.2	25.8±21.4
Ethylbenzene	0.3±0.2	0.4±0.5	0.1±0.1	0.2±0.1	0.7±0.3	4.4±2.7	6.3±7.7	0.9±0.8	3.0±1.0	9.5±4.8
m-Xylene	0.4±0.2	1.2±1.2	0.1±0.1	0.4±0.2	0.3±0.1	17.2±9.0	53.8±56.1	3.6±2.6	16.7±8.0	12.5±5.9
Styrene	0.5±0.4	0.8±1.1	0.1±0.0	0.3±0.3	0.6±0.4	3.7±3.4	6.8±8.5	0.6±0.3	2.3±2.5	4.6±3.0
o-Xylene	0.2±0.1	0.7±0.8	0.1±0.0	0.1±0.1	1.5±2.2	6.0±3.9	23.6±29.3	2.1±1.4	5.1±2.4	53.2±79.4
Isopropylbenzene	0.0±0.1	0.4±0.5	0.0±0.1	0.0±0.1	0.2±0.1	0.2±0.4	5.3±6.9	0.2±0.3	0.1±0.2	2.8±1.7
n-Propylbenzene	0.0±0.1	0.4±0.5	0.0±0.1	0.0±0.1	0.0±0.1	0.5±0.4	4.0±5.3	0.1±0.3	0.2±0.4	0.0±0.1
m-Ethyltoluene	0.1±0.1	0.0±0.1	0.0±0.1	0.0±0.1	0.0±0.1	4.1±1.8	0.0±0.1	1.0±1.2	1.0±1.5	0.3±0.6
p-Ethyltoluene	0.0±0.1	0.3±0.3	0.0±0.1	0.0±0.1	0.1±0.1	1.0±0.6	7.1±6.6	0.3±0.5	0.0±0.1	1.3±1.8
1,3,5-Trimethylbenzene	0.0±0.1	0.2±0.2	0.0±0.1	0.0±0.1	0.0±0.1	2.6±2.3	13.6±15.3	1.2±2.0	0.0±0.1	0.0±0.1
1,2,4-Trimethylbenzene	0.1±0.1	0.3±0.3	0.2±0.1	0.0±0.1	0.0±0.1	2.6±3.1	13.7±13.4	7.4±3.6	2.3±2.4	0.2±0.7
1,2,3-Trimethylbenzene	0.0±0.1	0.3±0.3	0.0±0.1	0.0±0.1	0.1±0.1	0.0±0.0	18.1±17.2	3.1±2.1	0.0±0.1	6.5±4.9
o-Ethyltoluene	0.0±0.1	0.2±0.2	0.0±0.1	0.0±0.1	0.0±0.1	1.2±1.4	7.0±7.0	0.8±0.8	0.6±0.9	0.7±0.9
m-Diethylbenzene	0.1±0.1	0.2±0.2	0.0±0.1	0.0±0.1	0.1±0.1	6.0±2.6	7.2±10.2	1.1±1.5	0.0±0.1	2.4±2.9

Species/Groups	VOC mixing ratios (mean±std) ( $\times 10^{-9}$ )					OFP (mean±std) ( $\mu\text{g m}^{-3}$ )				
	CD	CQ	TZ	XD	ZL	CD	CQ	TZ	XD	ZL
p-Diethylbenzene	0.1±0.1	0.2±0.2	0.0±0.1	0.0±0.1	0.1±0.1	2.0±1.4	4.1±5.5	0.3±0.5	0.0±0.1	2.7±1.1
Ethylene	1.4±1.2	1.8±0.9	1.6±1.2	1.4±0.6	2.7±1.4	15.5±13.6	20.4±9.6	17.9±13.1	15.3±6.7	29.9±15.3
Propylene	0.4±0.4	0.9±0.7	0.7±0.5	0.6±0.4	1.6±1.5	8.8±8.0	20.7±15.6	14.6±11.8	12.5±8.2	36.0±33.9
trans-2-Butene	0.1±0.1	0.0±0.1	0.0±0.1	0.2±0.2	0.4±0.2	2.0±2.4	0.0±0.1	1.6±2.5	6.5±7.8	14.0±8.5
1-Butene	0.0±0.1	0.0±0.1	0.0±0.1	0.1±0.2	0.2±0.2	1.2±1.6	1.0±1.1	1.0±1.7	3.2±4.1	5.0±3.7
cis-2-Butene	0.0±0.1	0.3±0.2	0.0±0.1	0.1±0.1	0.1±0.1	0.7±1.9	10.2±8.0	0.3±0.8	3.7±4.8	2.3±4.0
trans-2-Pentene	0.0±0.1	0.0±0.1	0.1±0.1	0.0±0.1	0.0±0.1	0.7±1.5	1.0±1.3	2.0±2.5	0.1±0.3	0.0±0.1
1-Pentene	0.0±0.1	0.1±0.1	0.0±0.1	0.0±0.1	0.2±0.2	0.2±0.7	1.8±1.3	0.9±1.6	0.5±0.6	3.9±4.8
cis-2-Pentene	0.0±0.1	0.1±0.1	0.3±0.3	0.0±0.1	0.0±0.1	0.0±0.1	1.9±3.2	10.6±9.5	0.3±0.9	0.6±1.4
1-Hexene	1.4±1.0	0.0±0.1	0.2±0.2	0.4±0.7	0.5±0.4	28.1±20.3	0.4±0.6	3.2±3.5	8.4±13.7	10.1±8.9
Ethane	4.0±1.5	3.3±1.6	4.4±3.9	2.4±0.8	0.0±0.1	1.5±0.6	1.2±0.6	1.7±1.5	0.9±0.3	0.0±0.1
Propane	2.8±1.7	3.9±2.4	13.3±11.1	4.1±2.3	3.2±0.8	2.7±1.6	3.7±2.3	12.8±10.7	4.0±2.2	3.1±0.8
Isobutane	0.8±0.6	1.4±1.4	1.0±1.2	1.3±1.1	3.2±1.4	2.6±1.9	4.5±4.6	3.2±3.9	4.1±3.4	10.3±4.5
n-Butane	1.6±0.9	2.4±2.4	4.4±3.6	2.9±2.5	0.9±0.5	4.7±2.8	7.0±7.2	13.0±10.9	8.7±7.6	2.7±1.6
Cyclopentane	0.1±0.1	0.3±0.2	2.5±2.2	0.3±0.5	1.6±0.9	0.3±0.3	0.9±0.8	8.9±7.8	1.2±1.7	5.9±3.1
Isopentane	1.3±0.7	0.4±0.8	0.0±0.1	8.6±5.0	0.1±0.1	10.3±5.5	3.4±5.9	0.0±0.1	66.2±38.5	0.6±0.5
n-Pentane	0.7±0.6	0.3±0.5	0.0±0.1	1.3±1.2	1.4±0.8	3.1±2.4	1.4±2.3	0.0±0.1	5.5±5.0	6.0±3.2
2,2-Dimethylbutane	0.1±0.1	0.1±0.1	0.0±0.1	0.0±0.1	0.8±0.6	0.6±0.6	0.4±0.6	0.2±0.5	0.0±0.1	3.8±2.7
2,3-Dimethylbutane	0.1±0.2	0.0±0.1	0.2±0.2	0.0±0.1	0.0±0.1	0.5±0.6	0.1±0.1	0.9±0.8	0.1±0.2	0.1±0.1
2-Methylpentane	0.2±0.1	0.2±0.2	0.0±0.1	0.4±0.3	0.4±0.2	0.9±0.8	1.0±0.9	0.0±0.1	2.4±1.8	2.0±0.9
3-Methylpentane	0.3±0.2	0.3±0.2	0.0±0.1	0.3±0.1	0.3±0.2	1.9±1.4	2.0±1.6	0.0±0.1	2.3±1.0	2.0±1.1
n-Hexane	0.6±0.4	0.2±0.3	0.0±0.1	0.6±0.2	0.1±0.1	2.7±2.0	0.9±1.4	0.1±0.4	2.7±1.1	0.4±0.4

Species/Groups	VOC mixing ratios (mean±std) ( $\times 10^{-9}$ )					OFP (mean±std) ( $\mu\text{g m}^{-3}$ )				
	CD	CQ	TZ	XD	ZL	CD	CQ	TZ	XD	ZL
Methylcyclopentane	0.1±0.1	0.1±0.2	0.0±0.0	0.0±0.1	0.7±0.5	0.9±0.9	0.9±1.3	0.0±0.1	0.1±0.5	5.5±3.8
2,4-Dimethylpentane	0.1±0.1	0.0±0.1	0.2±0.2	0.2±0.1	0.1±0.1	0.8±0.4	0.2±0.3	1.2±1.3	1.2±0.9	1.0±1.0
Cyclohexane	0.1±0.1	0.2±0.3	0.0±0.1	0.1±0.1	0.2±0.1	0.6±0.3	1.1±1.3	0.0±0.1	0.4±0.4	0.9±0.4
2-Methylhexane	0.0±0.1	0.0±0.1	0.0±0.1	0.1±0.1	0.0±0.1	0.2±0.3	0.3±0.3	0.0±0.1	0.3±0.3	0.2±0.3
3-Methylhexane	0.1±0.1	0.3±0.3	0.0±0.1	0.1±0.1	0.0±0.1	0.7±0.5	2.1±2.4	0.0±0.1	0.7±0.6	0.1±0.1
2,3-Dimethylpentane	0.0±0.1	0.1±0.1	0.1±0.1	0.1±0.1	0.1±0.1	0.0±0.1	0.6±0.7	0.8±0.8	0.4±0.5	0.7±0.3
2,2,4-Trimethylpentane	0.0±0.1	0.1±0.1	2.5±1.7	0.0±0.1	0.0±0.1	0.1±0.2	0.9±0.7	16.4±10.7	0.2±0.3	0.0±0.1
n-Heptane	0.1±0.1	0.4±0.3	0.6±0.4	0.2±0.1	0.0±0.1	0.4±0.4	2.1±1.6	2.8±2.1	0.8±0.4	0.2±0.2
Methylcyclohexane	0.0±0.1	0.2±0.2	0.0±0.1	0.1±0.1	0.1±0.1	0.2±0.4	1.3±1.5	0.2±0.5	1.0±0.9	0.7±0.6
2,3,4-Trimethylpentane	0.0±0.1	0.2±0.2	0.2±0.4	0.0±0.1	0.0±0.1	0.0±0.1	1.2±1.2	1.2±2.0	0.0±0.1	0.0±0.1
2-Methylheptane	0.0±0.1	0.2±0.2	0.0±0.1	0.0±0.1	0.1±0.1	0.0±0.1	1.1±1.1	0.2±0.5	0.1±0.1	0.3±0.4
3-Methylheptane	0.0±0.1	0.8±0.5	0.2±0.2	0.0±0.1	0.0±0.1	0.2±0.3	4.9±3.2	1.5±1.3	0.1±0.2	0.0±0.1
n-Octane	0.0±0.1	0.3±0.3	0.1±0.1	0.0±0.1	0.0±0.1	0.1±0.1	1.2±1.4	0.4±0.5	0.2±0.2	0.1±0.2
n-Nonane	0.0±0.1	0.2±0.2	0.0±0.1	0.0±0.1	0.0±0.1	0.1±0.1	0.9±1.0	0.1±0.3	0.2±0.2	0.1±0.2
n-Decane	0.0±0.1	0.2±0.3	0.0±0.1	0.0±0.1	0.0±0.1	0.0±0.1	0.9±1.4	0.1±0.1	0.0±0.1	0.1±0.1
n-Undecane	0.0±0.1	0.2±0.2	0.1±0.0	0.0±0.1	0.0±0.1	0.1±0.1	0.8±0.9	0.3±0.2	0.1±0.2	0.0±0.1
n-Dodecane	0.0±0.1	0.2±0.2	0.1±0.1	0.0±0.1	0.0±0.1	0.0±0.1	0.8±0.9	0.3±0.2	0.0±0.0	0.0±0.1
Formaldehyde	4.5±2.3	6.6±3.5	15.9±20.0	8.1±4.3	7.8±3.8	56.6±29.1	83.3±44.4	202.0±253.8	103.2±54.8	99.1±48.0
Acetaldehyde	2.1±1.7	3.1±2.1	2.4±1.1	4.3±3.4	2.1±0.7	27.6±21.4	39.4±27.5	31.0±14.7	55.6±44.2	27.4±8.8
Acetone	2.6±1.5	2.9±1.8	1.9±1.2	2.6±1.0	2.7±1.6	2.4±1.4	2.7±1.6	1.8±1.2	2.4±0.9	2.5±1.5
Acrolein	0.0±0.1	0.0±0.1	0.0±0.1	0.1±0.2	0.0±0.1	0.0±0.1	0.2±0.6	0.0±0.2	1.4±4.6	0.1±0.3
Propionaldehyde	0.3±0.1	0.4±0.2	0.3±0.1	0.4±0.3	0.3±0.1	5.0±2.4	7.3±3.9	5.5±2.1	7.5±5.2	5.6±2.2
Crotonaldehyde	0.1±0.1	0.1±0.2	0.0±0.1	0.1±0.1	0.1±0.2	1.8±3.1	2.4±5.9	0.2±0.6	1.8±2.8	3.9±4.9
Butyraldehyde	0.2±0.1	0.2±0.3	0.2±0.1	0.8±0.9	0.1±0.1	3.5±2.6	4.7±5.2	3.4±2.3	14.7±16.7	2.8±2.4

Species/Groups	VOC mixing ratios (mean±std) ( $\times 10^{-9}$ )					OFP (mean±std) ( $\mu\text{g m}^{-3}$ )				
	CD	CQ	TZ	XD	ZL	CD	CQ	TZ	XD	ZL
Benzaldehyde	0.1±0.1	0.2±0.1	0.2±0.1	0.3±0.6	0.2±0.1	-0.4±0.4	-0.8±0.4	-0.5±0.3	-1.0±1.9	-0.6±0.4
Cyclohexanone	0.0±0.1	0.1±0.2	0.1±0.1	0.1±0.1	0.2±0.2	0.1±0.2	0.9±0.9	0.7±0.6	0.5±0.4	1.1±1.2
Isovaleraldehyde	0.1±0.2	0.1±0.1	0.1±0.2	0.1±0.1	0.0±0.1	1.9±4.0	1.1±1.1	2.5±4.1	1.2±0.6	0.9±1.0
Pentanal	0.0±0.1	0.0±0.1	0.1±0.1	0.1±0.1	0.1±0.1	0.5±0.8	0.7±0.8	1.8±1.2	1.3±0.7	1.6±1.4
o-Tolualdehyde	0.0±0.1	0.0±0.1	0.0±0.1	0.0±0.1	0.0±0.1	0.0±0.0	0.0±0.0	0.0±0.0	0.0±0.0	0.0±0.0
m-Tolualdehyde	0.1±0.1	0.1±0.1	0.1±0.1	0.1±0.1	0.1±0.1	0.0±0.0	0.0±0.0	0.0±0.0	0.0±0.0	0.0±0.0
Hexaldehyde	0.1±0.2	0.2±0.2	0.3±0.2	0.3±0.2	0.2±0.2	2.7±3.0	2.9±4.0	4.9±3.2	4.9±3.3	3.5±3.7
Heptaldehyde	0.0±0.1	0.0±0.1	0.1±0.1	0.0±0.1	0.0±0.1	0.0±0.1	0.2±0.5	1.3±1.0	0.3±0.5	0.2±0.4
Octanal	0.0±0.1	0.1±0.1	0.1±0.1	0.1±0.1	0.1±0.1	0.6±1.3	1.4±1.3	1.6±1.4	1.2±1.0	1.3±1.4
Nonanal	0.3±0.2	0.3±0.1	0.3±0.3	0.3±0.1	0.3±0.1	0.0±0.0	0.0±0.0	0.0±0.0	0.0±0.0	0.0±0.0
Decanal	0.2±0.1	0.1±0.1	0.1±0.1	0.2±0.1	0.2±0.1	0.0±0.0	0.0±0.0	0.0±0.0	0.0±0.0	0.0±0.0

121  
122

**Table S6 Summary of main meteorological parameters and average levels of pollutants during the observation period.**

Parameters	CD	CQ	TZ	XD	ZL
WS (m/s)	2.1±1.2	2.0±1.0	1.9±1.0	1.9±1.1	1.5±1.0
T (°C)	27.3±2.9	28.2±2.9	27.1±3.1	27.4±3.3	27.3±3.4
RH (%)	69.1±11.8	70.4±13.1	85.4±17.0	74.6±13.9	70.9±14.9
P(hPa)	984.6±2.5	1005.2±2.6	1005.6±2.6	1001.6±2.6	996.1±2.5
BLH (m)	421.2±512.2	451.5±510.1	421.3±465.1	463.9±541.2	443.8±528.3
SSR (10 <sup>5</sup> J m <sup>-2</sup> )	6.7±8.3	6.5±8.1	6.3±7.7	6.6±8.2	6.6±8.2
NO (× 10 <sup>-9</sup> )	3.9±4.7	4.5±7.8	1.9±4.1	1.1±1.1	2.6±2.9
NO <sub>2</sub> (× 10 <sup>-9</sup> )	10.8±5.1	12.7±8.1	10.4±6.7	11.4±6.7	14.8±6.6
SO <sub>2</sub> (× 10 <sup>-9</sup> )	3.4±1.3	3.0±0.5	2.2±1.6	1.4±1.3	3.9±1.5
CO (× 10 <sup>-9</sup> )	508.0±173.6	1176.4±578.4	674.3±190.9	1261.4±1174.1	868.0±258.3
O <sub>3</sub> (× 10 <sup>-9</sup> )	58.6±30.0	56.4±34.2	51.0±27.8	56.1±29.4	57.4±32.2

123  
124

**Table S7 Modeled O<sub>3</sub> assessment of Base and Free scenario.**

Site	Base		Free	
	IOA	R	IOA	R
CD	0.80	0.88	0.90	0.88
CQ	0.90	0.87	0.86	0.87
TZ	0.88	0.88	0.85	0.88
XD	0.86	0.88	0.83	0.89
ZL	0.88	0.89	0.88	0.87

125  
126  
127

**Table S8 Comparison concentrations of the Base and Free scenario modeling parameters, including OVOCs, O<sub>3</sub>, RO<sub>2</sub>, HO<sub>2</sub>, and OH at the five sites.**

Parameter	site	Conc		Parameter	site	Conc	
		Base	Free			Base	Free
OVOCs	CD	10.3	18.7	Daytime OH	CD	3.87E+06	3.06E+06
	CQ	14.0	26.3		CQ	2.78E+06	2.64E+06
	TZ	21.9	21.9		TZ	2.99E+06	2.94E+06
	XD	17.4	24.7		XD	3.10E+06	3.01E+06
	ZL	14.2	32.1		ZL	3.56E+06	3.20E+06
Daytime O <sub>3</sub>	CD	60.9	68.2	Daytime HO <sub>2</sub>	CD	4.13E+08	4.67E+08
	CQ	82.4	84.1		CQ	7.75E+08	8.58E+08
	TZ	66.2	68.8		TZ	7.56E+08	7.96E+08

	XD	85.2	86.7		XD	6.45E+08	7.34E+08
	ZL	96.8	106.3		ZL	7.26E+08	8.74E+08
Daytime   $\Delta O_3$	CD	18.1	14.6	Daytime RO <sub>2</sub>	CD	3.67E+08	4.96E+08
	CQ	18.0	18.1		CQ	8.25E+08	8.79E+08
	TZ	12.3	13.1		TZ	6.74E+08	7.29E+08
	XD	18.6	19.8		XD	6.79E+08	7.26E+08
	ZL	21.0	29.1		ZL	7.26E+08	8.72E+08

Note: Concentrations of OVOCs and O<sub>3</sub> in  $\times 10^{-9}$ , RO<sub>2</sub>, HO<sub>2</sub> and OH in molecules cm<sup>-3</sup>.; | $\Delta O_3$ | = |Sim – Obs|.

128 **Table S9 Model sensitivity testing due to HONO mixing ratios. The change is based on a**  
 129 **ratio of HONO/NO<sub>2</sub> of 0.02.**

HONO/NO <sub>2</sub> ratio	Change in O <sub>3</sub>	Change in OH	Change in HO <sub>2</sub>	Change in RO <sub>2</sub>
0.005	-3.4%	-4.6%	-4.8%	-6.0%
0.01	-2.2%	-3.0%	-3.1%	-4.0%
0.03	2.0%	2.7%	2.8%	3.6%
0.04	3.8%	5.4%	5.6%	7.2%

130

131 **Table S10 Changes in R<sub>NetProd</sub>, R<sub>Emis&Trans</sub>, and R<sub>Deps</sub> contributions to OVOC in different**  
 132 **time-step scenarios relative to the Base scenario (1-hour time-step).**

Time-step	R <sub>NetProd</sub>	R <sub>Emisa&amp;Trans</sub>	R <sub>Deps</sub>
5 minutes	4.3%	5.0%	-0.2%
10 minutes	4.2%	4.8%	-0.1%
30 minutes	2.8%	3.2%	-0.1%

133

134 **Table S11 The one-way analysis of variance (ANOVA) results for pollutants level, OFP of**  
 135 **different VOC groups, and daytime contributions of OVOC budget.**

Type	Group	F-stat <sup>a</sup>	p-value <sup>b</sup>
Mixing ratio	O <sub>3</sub>	1.08	3.66E-01
	NO <sub>2</sub>	8.52	1.09E-06
	NO	10.74	2.07E-08
	CO	33.52	3.09E-25
	TVOCs	8.78	1.35E-06
OFP	OVOCs	8.28	3.06E-06
	Aromatics	28.56	4.06E-19
	Alkanes	28.23	6.21E-19
	Alkenes	15.48	3.55E-11
	BVOCs	13.11	1.36E-09
	Alkyne	39.91	4.09E-25
	TVOCs	8.10	4.15E-06
Daytime	R <sub>NetProd</sub>	14.87	5.42E-11
OVOC	R <sub>Deps</sub>	4.13	2.89E-03
budget	R <sub>Emis&amp;Trans</sub>	10.74	4.35E-08

Note: <sup>a</sup> F-statistic (F-stat) measures the ratio of OFP variance between VOC groups to the variance within the groups. A higher F-stat indicates a larger difference between the groups relative to the variation within the groups. This suggests that OFP is more likely to differ across VOCs categories.

<sup>b</sup> p-value indicates the probability that the observed difference (or a more extreme difference) occurred by chance. A p-value less than 0.05 typically indicates that the observed differences are statistically significant, meaning there is a high likelihood that the differences are not due to random variation.

136



137 **Reference**

- 138 Chen, G., Liu, T., Chen, J., Xu, L., Hu, B., Yang, C., Fan, X., Li, M., Hong, Y., Ji, X., Chen, J., and  
139 Zhang, F.: Atmospheric oxidation capacity and O<sub>3</sub> formation in a coastal city of southeast China:  
140 Results from simulation based on four-season observation, *J. Environ. Sci.*, 136, 68–80,  
141 <https://doi.org/10.1016/j.jes.2022.11.015>, 2024.
- 142 Del Negro, L. A., Fahey, D. W., Gao, R. S., Donnelly, S. G., Keim, E. R., Neuman, J. A., Cohen,  
143 R. C., Perkins, K. K., Koch, L. C., Salawitch, R. J., Lloyd, S. A., Proffitt, M. H., Margitan, J. J.,  
144 Stimpfle, R. M., Bonne, G. P., Voss, P. B., Wennberg, P. O., McElroy, C. T., Swartz, W. H.,  
145 Kusterer, T. L., Anderson, D. E., Lait, L. R., and Bui, T. P.: Comparison of modeled and observed  
146 values of NO<sub>2</sub> and JNO<sub>2</sub> during the Photochemistry of Ozone Loss in the Arctic Region in  
147 Summer (POLARIS) mission, *J. Geophys. Res.-Atmos.*, 104, 26687–26703,  
148 <https://doi.org/10.1029/1999JD900246>, 1999.
- 149 Gu, Y., Liu, B., Li, Y., Zhang, Y., Bi, X., Wu, J., Song, C., Dai, Q., Han, Y., Ren, G., and Feng, Y.:  
150 Multi-scale volatile organic compound (VOC) source apportionment in Tianjin, China, using a  
151 receptor model coupled with 1-hr resolution data, *Environ. Pollut.*, 265, 115023,  
152 <https://doi.org/10.1016/j.envpol.2020.115023>, 2020.
- 153 Han, Y., Huang, X., Wang, C., Zhu, B., and He, L.: Characterizing oxygenated volatile organic  
154 compounds and their sources in rural atmospheres in China, *J. Environ. Sci.*, 81, 148–155,  
155 <https://doi.org/10.1016/j.jes.2019.01.017>, 2019.
- 156 Hong, Z., Li, M., Wang, H., Xu, L., Hong, Y., Chen, J., Chen, J., Zhang, H., Zhang, Y., Wu, X., Hu,  
157 B., and Li, M.: Characteristics of atmospheric volatile organic compounds (VOCs) at a  
158 mountainous forest site and two urban sites in the southeast of China, *Sci. Total Environ.*, 657,  
159 1491–1500, <https://doi.org/10.1016/j.scitotenv.2018.12.132>, 2019.
- 160 Huang, X.-F., Wang, C., Zhu, B., Lin, L.-L., and He, L.-Y.: Exploration of sources of OVOCs in  
161 various atmospheres in southern China, *Environ. Pollut.*, 249, 831–842,  
162 <https://doi.org/10.1016/j.envpol.2019.03.106>, 2019.
- 163 Hui, L., Liu, X., Tan, Q., Feng, M., An, J., Qu, Y., Zhang, Y., and Jiang, M.: Characteristics, source  
164 apportionment and contribution of VOCs to ozone formation in Wuhan, Central China, *Atmos.*  
165 *Environ.*, 192, 55–71, <https://doi.org/10.1016/j.atmosenv.2018.08.042>, 2018.
- 166 Jaeglé, L., Webster, C. R., May, R. D., Fahey, D. W., Woodbridge, E. L., Keim, E. R., Gao, R. S.,  
167 Proffitt, M. H., Stimpfle, R. M., Salawitch, R. J., Wofsy, S. C., and Pfister, L.: In situ  
168 measurements of the NO<sub>2</sub>/NO ratio for testing atmospheric photochemical models, *Geophysical*  
169 *Research Letters*, 21, 2555–2558, <https://doi.org/10.1029/94GL02717>, 1994.
- 170 Kim, S., Kim, S.-Y., Lee, M., Shim, H., Wolfe, G. M., Guenther, A. B., He, A., Hong, Y., and Han,  
171 J.: Impact of isoprene and HONO chemistry on ozone and OVOC formation in a semirural South  
172 Korean forest, *Atmos. Chem. Phys.*, 15, 4357–4371, <https://doi.org/10.5194/acp-15-4357-2015>,  
173 2015.
- 174 Li, C., Liu, Y., Cheng, B., Zhang, Y., Liu, X., Qu, Y., An, J., Kong, L., Zhang, Y., Zhang, C., Tan,  
175 Q., and Feng, M.: A comprehensive investigation on volatile organic compounds (VOCs) in 2018  
176 in Beijing, China: Characteristics, sources and behaviours in response to O<sub>3</sub> formation, *Sci. Total*  
177 *Environ.*, 806, 150247, <https://doi.org/10.1016/j.scitotenv.2021.150247>, 2022.
- 178 Li, J., Zhai, C., Yu, J., Liu, R., Li, Y., Zeng, L., and Xie, S.: Spatiotemporal variations of ambient  
179 volatile organic compounds and their sources in Chongqing, a mountainous megacity in China,  
180 *Sci. Total Environ.*, 627, 1442–1452, <https://doi.org/10.1016/j.scitotenv.2018.02.010>, 2018.

181 Li, K., Wang, X., Li, L., Wang, J., Liu, Y., Cheng, X., Xu, B., Wang, X., Yan, P., Li, S., Geng, C.,  
182 Yang, W., Azzi, M., and Bai, Z.: Large variability of O<sub>3</sub>-precursor relationship during severe  
183 ozone polluted period in an industry-driven cluster city (Zibo) of North China Plain, *J. Clean*  
184 *Prod.*, 316, 128252, <https://doi.org/10.1016/j.jclepro.2021.128252>, 2021.

185 Li, X., Rohrer, F., Brauers, T., Hofzumahaus, A., Lu, K., Shao, M., Zhang, Y. H., and Wahner, A.:  
186 Modeling of HCHO and CHOCHO at a semi-rural site in southern China during the PRIDE-  
187 PRD2006 campaign, *Atmos. Chem. Phys.*, 14, 12291–12305, [https://doi.org/10.5194/acp-14-](https://doi.org/10.5194/acp-14-12291-2014)  
188 12291-2014, 2014.

189 Li, Y., Yin, S., Yu, S., Yuan, M., Dong, Z., Zhang, D., Yang, L., and Zhang, R.: Characteristics,  
190 source apportionment and health risks of ambient VOCs during high ozone period at an urban  
191 site in central plain, China, *Chemosphere*, 250, 126283,  
192 <https://doi.org/10.1016/j.chemosphere.2020.126283>, 2020.

193 Liu, Y., Shen, H., Mu, J., Li, H., Chen, T., Yang, J., Jiang, Y., Zhu, Y., Meng, H., Dong, C., Wang,  
194 W., and Xue, L.: Formation of peroxyacetyl nitrate (PAN) and its impact on ozone production in  
195 the coastal atmosphere of Qingdao, North China, *Sci. Total Environ.*, 778, 146265,  
196 <https://doi.org/10.1016/j.scitotenv.2021.146265>, 2021a.

197 Liu, Y., Wang, H., Jing, S., Peng, Y., Gao, Y., Yan, R., Wang, Q., Lou, S., Cheng, T., and Huang,  
198 C.: Strong regional transport of volatile organic compounds (VOCs) during wintertime in  
199 Shanghai megacity of China, *Atmos. Environ.*, 244, 117940,  
200 <https://doi.org/10.1016/j.atmosenv.2020.117940>, 2021b.

201 Liu, Y., Qiu, P., Xu, K., Li, C., Yin, S., Zhang, Y., Ding, Y., Zhang, C., Wang, Z., Zhai, R., Deng,  
202 Y., Yan, F., Zhang, W., Xue, Z., Sun, Y., Ji, D., Li, J., Chen, J., Tian, H., Liu, X., and Zhang, Y.:  
203 Analysis of VOC emissions and O<sub>3</sub> control strategies in the Fenhe Plain cities, China, *J. Environ.*  
204 *Manage.*, 325, 116534, <https://doi.org/10.1016/j.jenvman.2022.116534>, 2023.

205 Ma, Z., Liu, C., Zhang, C., Liu, P., Ye, C., Xue, C., Zhao, D., Sun, J., Du, Y., Chai, F., and Mu, Y.:  
206 The levels, sources and reactivity of volatile organic compounds in a typical urban area of  
207 Northeast China, *J. Environ. Sci.*, 79, 121–134, <https://doi.org/10.1016/j.jes.2018.11.015>, 2019.

208 Simayi, M., Shi, Y., Xi, Z., Li, J., Yu, X., Liu, H., Tan, Q., Song, D., Zeng, L., Lu, S., and Xie, S.:  
209 Understanding the sources and spatiotemporal characteristics of VOCs in the Chengdu Plain,  
210 China, through measurement and emission inventory, *Sci. Total Environ.*, 714, 136692,  
211 <https://doi.org/10.1016/j.scitotenv.2020.136692>, 2020.

212 Song, M., Tan, Q., Feng, M., Qu, Y., Liu, X., An, J., and Zhang, Y.: Source Apportionment and  
213 Secondary Transformation of Atmospheric Nonmethane Hydrocarbons in Chengdu, Southwest  
214 China, *J. Geophys. Res.-Atmos.*, 123, 9741–9763, <https://doi.org/10.1029/2018JD028479>, 2018.

215 Song, M., Li, X., Yang, S., Yu, X., Zhou, S., Yang, Y., Chen, S., Dong, H., Liao, K., Chen, Q., Lu,  
216 K., Zhang, N., Cao, J., Zeng, L., and Zhang, Y.: Spatiotemporal variation, sources, and secondary  
217 transformation potential of volatile organic compounds in Xi'an, China, *Atmos. Chem. Phys.*, 21,  
218 4939–4958, <https://doi.org/10.5194/acp-21-4939-2021>, 2021.

219 Tan, Z., Fuchs, H., Lu, K., Hofzumahaus, A., Bohn, B., Broch, S., Dong, H., Gomm, S., Haeseler,  
220 R., He, L., Holland, F., Li, X., Liu, Y., Lu, S., Rohrer, F., Shao, M., Wang, B., Wang, M., Wu,  
221 Y., Zeng, L., Zhang, Y., Wahner, A., and Zhang, Y.: Radical chemistry at a rural site (Wangdu)  
222 in the North China Plain: observation and model calculations of OH, HO<sub>2</sub> and RO<sub>2</sub> radicals,  
223 *Atmos. Chem. Phys.*, 17, 663–690, <https://doi.org/10.5194/acp-17-663-2017>, 2017.

224 Tan, Z., Lu, K., Jiang, M., Su, R., Wang, H., Lou, S., Fu, Q., Zhai, C., Tan, Q., Yue, D., Chen, D.,  
225 Wang, Z., Xie, S., Zeng, L., and Zhang, Y.: Daytime atmospheric oxidation capacity in four  
226 Chinese megacities during the photochemically polluted season: a case study based on box model  
227 simulation, *Atmos. Chem. Phys.*, 19, 3493–3513, <https://doi.org/10.5194/acp-19-3493-2019>,  
228 2019.

229 Wang, N., Li, N., Liu, Z., and Evans, E.: Investigation of chemical reactivity and active components  
230 of ambient VOCs in Jinan, China, *Air Qual Atmos Health*, 9, 785–793,  
231 <https://doi.org/10.1007/s11869-015-0380-1>, 2016.

232 Wang, X., Yin, S., Zhang, R., Yuan, M., and Ying, Q.: Assessment of summertime O<sub>3</sub> formation  
233 and the O<sub>3</sub>-NO<sub>x</sub>-VOC sensitivity in Zhengzhou, China using an observation-based model, *Sci.*  
234 *Total Environ.*, 813, 152449, <https://doi.org/10.1016/j.scitotenv.2021.152449>, 2022.

235 Xu, K., Liu, Y., Li, C., Zhang, C., Liu, X., Li, Q., Xiong, M., Zhang, Y., Yin, S., and Ding, Y.:  
236 Enhanced secondary organic aerosol formation during dust episodes by photochemical reactions  
237 in the winter in Wuhan, *J. Environ. Sci.*, 133, 70–82,  
238 <https://doi.org/10.1016/j.jes.2022.04.0181001-0742>, 2023.

239 Xu, Z., Wang, T., Xue, L. K., Louie, P. K. K., Luk, C. W. Y., Gao, J., Wang, S. L., Chai, F. H., and  
240 Wang, W. X.: Evaluating the uncertainties of thermal catalytic conversion in measuring  
241 atmospheric nitrogen dioxide at four differently polluted sites in China, *Atmos. Environ.*, 76,  
242 221–226, <https://doi.org/10.1016/j.atmosenv.2012.09.043>, 2013.

243 Yang, Y., Shao, M., Keßel, S., Li, Y., Lu, K., Lu, S., Williams, J., Zhang, Y., Zeng, L., Nölscher,  
244 A. C., Wu, Y., Wang, X., and Zheng, J.: How the OH reactivity affects the ozone production  
245 efficiency: case studies in Beijing and Heshan, China, *Atmos. Chem. Phys.*, 17, 7127–7142,  
246 <https://doi.org/10.5194/acp-17-7127-2017>, 2017.

247 Yang, Y., Wang, Y., Huang, W., Yao, D., Zhao, S., Wang, Y., Ji, D., Zhang, R., and Wang, Y.:  
248 Parameterized atmospheric oxidation capacity and speciated OH reactivity over a suburban site  
249 in the North China Plain: A comparative study between summer and winter, *Sci. Total Environ.*,  
250 773, 145264, <https://doi.org/10.1016/j.scitotenv.2021.145264>, 2021.

251 Zhang, Z., Sun, Y., and Li, J.: Characteristics and sources of VOCs in a coastal city in eastern China  
252 and the implications in secondary organic aerosol and O<sub>3</sub> formation, *Sci. Total Environ.*, 887,  
253 164117, <https://doi.org/10.1016/j.scitotenv.2023.164117>, 2023.

254